European Journal of Medicinal Chemistry 178 (2019) 515–529

Contents lists available at ScienceDirect

European Journal of Medicinal Chemistry

journal homepage: http://www.elsevier.com/locate/ejmech

Research paper

Carvacrol prodrugs as novel antimicrobial agents

Lisa Marinelli [a], Erika Fornasari [a], Piera Eusepi [a], Michele Ciulla [a], Salvatore Genovese [a], Francesco Epifano [a], Serena Fiorito [a], Hasan Turkez [b], Serkan Örtücü [b], Marina Mingoia [c], Serena Simoni [c], Armanda Pugnaloni [d], Antonio Di Stefano [a], Ivana Cacciatore [a, *]

[a] Department of Pharmacy, "G. D'Annunzio" University of Chieti-Pescara, 66100, Chieti Scalo, CH, Italy
[b] Department of Molecular Biology and Genetics, Faculty of Science, Erzurum Technical University, Erzurum, Turkey
[c] Department of Biomedical Sciences and Public Health, Polytechnic University of Marche, via Tronto 10/A, 60020, Ancona, Italy
[d] Department of Clinical and Molecular Sciences, Polytechnic University of Marche, via Tronto 10/A, 60020, Ancona, Italy

ARTICLE INFO

Article history:
Received 16 April 2019
Received in revised form
31 May 2019
Accepted 31 May 2019
Available online 10 June 2019

Keywords:
Antimicrobial agent
Biofilm
Carvacrol
Prodrug

ABSTRACT

Carvacrol (CAR), a natural monoterpene particularly abundant in plants belonging to the Lamiaceae family, has recently attracted much attention for its many biological properties (antioxidant, anti-inflammatory, neuroprotective, antitumour, antibacterial, and several others). However, CAR has poor chemical-physical properties (low water solubility and high volatility), which hamper its potential pharmacological uses.

In this paper, the synthesis and antimicrobial evaluation of 23 carvacrol derivatives (**WSCP1-23**) against a panel of selected gram-positive and gram-negative bacteria are reported. Using the prodrug approach, CAR hydrophilic (**WSCP1-17**) and lipophilic prodrugs (**WSCP18–23**) were prepared. Notably, CAR water solubility was increased by using polar neutral groups (such as natural amino acids) with the aim of improving oral drug delivery. On the other hand, CAR lipophilic prodrugs, obtained by prenylation of CAR hydroxyl group, were designed to promote membrane permeation and oral absorption.

Our results revealed that **WSCP1-3**, showing the highest water solubility (>1700-fold compared to that of CAR), possessed good antibacterial activity against gram-negative bacteria with MIC values comparable to those of CAR and antifungal properties against different species of *Candida*. **WSCP18–19** were the most promising prodrugs, showing good antibacterial profiles against gram-positive bacteria by interfering with the biofilm formation of *Staphylococcus aureus* and *Staphylococcus epidermidis*. Moreover, **WSCP18–19** resulted more stable in simulated fluids and human plasma than **WSCP1-3**. Toxicity studies performed on human erythrocytes and HaCaT cells revealed that all **WSCPs** were not toxic at the tested concentrations.

1. Introduction

Infectious diseases are responsible for over 15 million deaths a year [1]. The high mortality rate is due to the widespread use of antibiotics in humans, which causes increased resistance by bacterial strains [2]. Biofilm formation, inactivation of antibiotics, alteration of target sites, and presence of efflux pumps denote the mechanisms by which bacteria have developed resistance to drugs [3]. To date, discovering new molecular entities able to overcome antibiotic resistance is very difficult, and many efforts are focused on enhancing the antibacterial activity of well-known natural products with low molecular weight [4].

Carvacrol (CAR, Chart 1) has recently attracted much attention because of its ability to inhibit the growth of preformed biofilms and to interfere with biofilm formation produced by bacteria [5]. Biofilms, which are a community of bacteria embedded in a self-produced matrix comprising polysaccharides, proteins, and DNA, are responsible for a great number of chronic infections in humans [6]. Notably, CAR acts on biofilms produced by gram-positive bacteria, especially *Staphylococcus aureus* and *Staphylococcus epidermidis*, leading to an increase in the fluidity, permeability, and

Abbreviations: AcOH, acetic acid; CAR, carvacrol; DCHA, Dicyclohexylamine; EDC·HCl, *N*-(3-dimethylaminopropyl)-N′-ethylcarbodiimide hydrochloride; HOBt, 1-Hydroxybenzotriazole; IBCF, isobutyl chloroformate; TEA, triethylamine; WSCP, water-soluble carvacrol prodrug.

* Corresponding author. Department of Pharmacy, "G. d'Annunzio" University of Chieti-Pescara, Via dei Vestini 31, 66100, Chieti Scalo, CH, Italy.
E-mail address: ivana.cacciatore@unich.it (I. Cacciatore).

https://doi.org/10.1016/j.ejmech.2019.05.093
0223-5234/

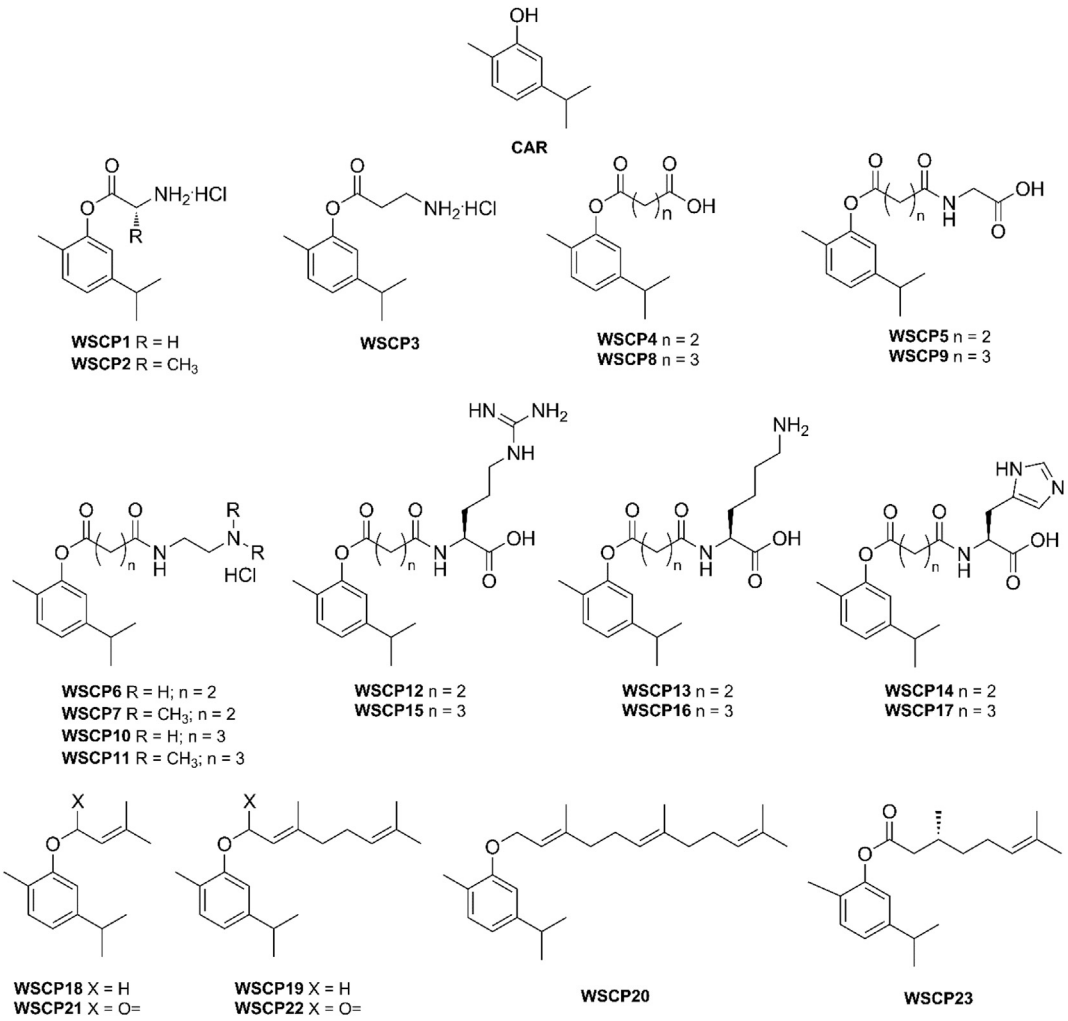

Chart 1. Chemical structures of CAR prodrugs (**WSCP1-23**).

perturbation of the lipid fractions of microbial cytoplasmatic membranes [7]. Unlike other phenol monoterpenes, CAR disintegrates the outer membrane of gram-negative bacteria [8].

From a chemical point of view, the presence of the hydroxyl group and a delocalized electron system are the structural requirements for the antibacterial activity of CAR [9]. The amphipathic structure of CAR allows it to spread through the polar matrix of biofilm produced by bacteria and to interact with lipids in the bacterial membrane causing disruption and loss of integrity [10]. However, some reports suggested that the derivatization of the CAR hydroxyl group with a phosphate moiety did not cause the loss of biological activity supporting the hypothesis that the hydroxyl group is not an essential requirement for the observed antibacterial activity [11].

Unfortunately, CAR has poor chemical-physical properties such as water solubility (0.11 mg/mL), high volatility, and low chemical stability, which hamper its therapeutic use in medicine. Water solubility is one of the parameters that limit the bioavailability of CAR since high doses of CAR are required to reach therapeutic plasma concentrations [12].

In the field of medicinal chemistry, the prodrug approach is an effective strategy to improve drug solubility [13]. Prodrugs are inactive molecules that can undergo biotransformation following chemical or enzymatic hydrolysis, releasing the parent molecule [14]. In our study, this approach was employed in the rational drug design of novel amino-acid-ester prodrugs (**WSCP1-17**) to improve CAR solubility while retaining the antibacterial activity. Notably, amino acids were used as water-soluble pro-moieties to design both bipartite (the carrier is directly linked to the parent molecule) and tripartite (the carrier and the parent molecule are separated by a linker) prodrugs [15]. The solubilizing moiety was conjugated by a covalent linkage to the CAR hydroxyl group, allowing the preparation of esterified CAR prodrugs (Chart 1) [16]. Succinic and glutaric acids were chosen as linkers, since the literature has well documented their capabilities to improve the crossing of bacterial lipid membrane [17]. Furthermore, CAR amino-acid-ester prodrugs could be better absorbed after oral administration than the parent drug due to the presence of several amino acid and small peptide membrane carriers located in the external portion of the intestinal brush border [18]. On the other hand, with the aim of improving membrane permeation and oral absorption, lipophilic prodrugs **WSCP18–23** were designed and synthetized. Prenylation was chosen in the development of novel CAR prodrugs since the addition of prenyl chains affects positively antimicrobial activities of natural compounds [19]. The prenylated chains (isopentenyl, geranyl, and farnesyl) were directly conjugated to the hydroxyl group of CAR through ether (**WSCP18–20**) or ester (**WSCP 21–23**) junction. The introduction of a prenyl chain into the molecule enhances its lipophilicity thus ameliorating affinity, interaction, and access with the bacterial membrane.

Here, we report the syntheses and antimicrobial and antifungal activities of a small library of CAR prodrugs (**WSCP 1**–**23**) (Chart 1). In addition, enzymatic and plasma stability studies were performed to evaluate the chemical-physical properties of the most promising prodrugs. Toxicity studies were also performed on human erythrocytes and HaCaT cells to evaluate the safety of the synthetized prodrugs.

2. Results and discussion

2.1. Design and synthesis of the compounds

In the first part of the work, the prodrug approach was used in the rational drug design to improve CAR water solubility (Schemes 1–3). In our synthetic strategy, the CAR hydroxyl group was conjugated both directly to the carboxylic moiety of amino acids (bipartite prodrugs, **WSCP1-4** and **8**) and by means of a linear linker (tripartite prodrugs, **WSCP5-7** and **9**–**17**). Succinic and glutaric acids were chosen as linkers to obtain the tripartite prodrugs [20]. In physiological conditions (pH 7.4), the prodrug undergoes enzymatic hydrolysis, releasing the parent drug [21]. Obviously, **WSCPs** can release the parent drug by chemical reaction that is dependent on the cyclization tendency of the spacer. The **WSCPs** were coupled with a suitable amino acid or linker by common coupling reagents. Glycine, alanine, and a basic amino acid (His, Arg, or Lys) were selected as natural amino acids.

In the second part of the work, prenylated chains were conjugated to the CAR hydroxyl group via an ether (**WSCP18**–**20**) or ester link (**WSCP21**–**23**) (Schemes 4 and 5). CAR was prenylated since prenylated phenolic compounds significantly correlated with antibacterial activity [22].

The first series of bipartite prodrugs, **WSCP 1**–**3**, was obtained through direct coupling of the CAR hydroxyl group with a suitable Boc-protected amino acid (Boc-Gly-OBu^t, Boc-Ala-OBu^t, or Boc-b-Ala-OBu^t) by employing *N*,*N*′-dicyclohexylcarbodiimide (DCC) at 0 °C for 3 h. Then, the final compounds, **WSCP1-3**, were easily obtained after treatment of the Boc-derivatives with gaseous hydrochloric acid at 0 °C for 1 h (Scheme 1).

Due to the diverse nature of WSCPs structures, several synthetic strategies were required, including the employment of different coupling agents or protection/deprotection steps. In the second series of prodrugs (Scheme 2), cyclic anhydrides (succinic and glutaric) were conjugated to CAR via condensation at room temperature in the presence of dicyclohexylamine (DCHA) to afford **WSCP4** and **WSCP8**, respectively, in good yields. Subsequently, **WSCP4** and **WSCP8** were conjugated, in a second coupling step, with other natural amino acids (Gly, Arg, Lys, and His suitably protected on the carboxy terminal group) to provide **WSCP5**, **WSCP9**, and **WSCP12**–**17** after deprotection of the carboxy terminal moieties with TFA (trifluoroacetic acid) or H_2 (Scheme 2).

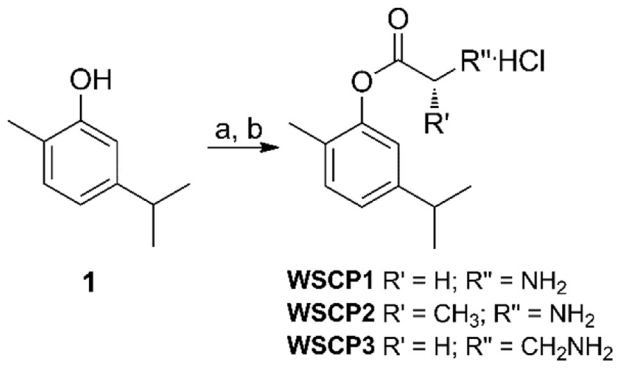

Scheme 1. Synthesis of **WSCP1-3**. *Reagents and conditions*: a) Boc-Gly-OBu^t·HCl (for the synthesis of **WSCP1**), Boc-L-Ala-OBu^t·HCl (for the synthesis of **WSCP2**), or Boc-L-β-Ala-OBu^t·HCl (for the synthesis of **WSCP3**), TEA, DCC, HOBt, dry DMF, 0 °C, 3 h, and rt, 15 h; b) HCl (g), dry EtOAc, 0 °C, 1 h, and rt, 3 h.

The third series of prodrugs, **WSCP7** and **11** were obtained after treatment of **WSCP4** or **WSCP8**, respectively, with *N*,*N*-dimethylethylenediamine in the presence of *N*-(3-dimethylaminopropyl)-N′-ethylcarbodiimide hydrochloride (EDC·HCl) while **WSCP6** and **10** were afforded after coupling with Boc-ethylenediamine and subsequent treatment in an acidic environment (deprotection of Boc-group with hydrochloric acid) (Scheme 3).

Moreover, CAR was converted into **WSCP21**–**23** by esterification reaction with a suitable acid chloride in the presence of Et_3N at rt for 2–5 h (Scheme 5). In addition to the esterified prodrugs, a series of etherified prodrugs were also synthetized to determine if the permanent ether linkage, not sensitive to the enzymatic action, could further improve antibacterial activity. Thus, the series of **WSCP18**–**20** were obtained after treatment of CAR with the suitable alkylating agent in the presence of K_2CO_3 at 80 °C for 2 h (Scheme 4).

2.2. Chemical-physical properties of WSCP1-23

The water-solubility of **WSCP1-23** was determined by HPLC and compared to that of the parent drug (Fig. 1). The results showed that **WSCP1-3** displayed high solubility (approximately 5300-, 1700-, and 4300-fold, respectively) compared to that of CAR, suggesting that salt formation remains the most common method to increase the solubility of drugs [23]. **WSCP6** and **16** were water soluble (360 and 700 times more than CAR, respectively) while other compounds were classified as poor or slightly soluble. The introduction of the linkers between the CAR hydroxyl group and the ethylenediamine chain increased the lipophilicity of the prodrugs (**WSCP4-11**), while the conjugation of the linkers to basic amino acids, such as Arg, Lys, or His (**WSCP12**–**17**), reduced the hydrophobic profile of the synthetized molecules (LogP < 2.4). As we expected, the prenylated prodrugs (**WSCP18**–**23)** were insoluble in water, and the lipophilic properties of the prodrugs were enhanced with the elongation of the alkyl chain. In fact, **WSCP20**, containing a farnesyl moiety, was the most hydrophobic prodrug showing LogP values (approximately 3-fold) higher than those of CAR.

2.3. Antibacterial testing of WSCP1-23

The antimicrobial activity of **WSCP1-23**, determined against a panel of gram-positive and gram-negative organisms, is expressed as minimum inhibitory concentration (MIC). The MIC values of CAR and **WSCP1**–**23** prodrugs are reported in Table 1. The species considered for this study include the gram-positive *Staphylococcus aureus*, *Staphylococcus epidermidis*, *Enterococcus faecalis*, *Streptococcus agalactiae*, *Streptococcus pyogenes*, and *Streptococcus pneumoniae;* and the gram-negative *Escherichia coli*, *Klebsiella pneumoniae*, *Pseudomonas aeruginosa*, and *Acinetobacter baumannii*.

WSCP1-3 showed antimicrobial activity mainly against the gram-negative species, especially *A. baumannii*, with a MIC value (128 μg/mL) comparable to that of CAR. On the other hand, **WSCP18**–**19** exhibited good activity against gram-positive species, notably against *S. pneumoniae* (MIC = 64 μg/mL for **WSCP18** and 16 μg/mL for **WSCP19**) and *E. faecalis* (MIC = 128 μg/mL for **WSCP18** and 64 μg/mL for **WSCP19**), compared to that of CAR (MIC = 256 μg/mL for both species). **WSCP18**–**19** did not show an effect on gram-negative species. **WSCP4-17** and **20**–**23** showed MIC values higher than that of CAR so they were not considered for further

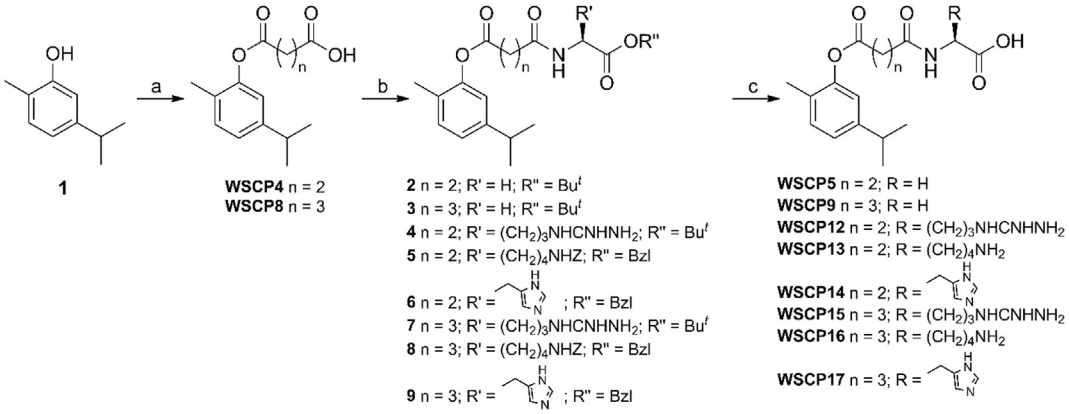

Scheme 2. Synthesis of **WSCP4-5, 8–9, 12–17**. *Reagents and conditions:* a) Succinic anhydride (for the synthesis of **WSCP4**) or glutaric anhydride (for the synthesis of **WSCP8**), DCHA, THF/Et_2O 1:2, rt, 24 h; b) H-Gly-OBu^t·HCl (**2** and **3**), or H-L-Arg-OBu^t·HCl (**4** and **7**), or H-L-Lys(Z)-OBzl·HCl (**5** and **8**), or H-L-His-OBzl·2HCl (**6** and **9**), TEA, DCC, HOBt, dry DMF, 0 °C, 3 h, and rt, 15 h; c) TFA, rt, 4 h (for the syntheses of **WSCP5**, **WSCP9**, **WSCP12**, and **WSCP15**); H_2 (g), Pd/C (30%), dry MeOH, AcOH (1%), rt, 6 h (for the syntheses of **WSCP13**, **WSCP14**, **WSCP16**, and **WSCP17**).

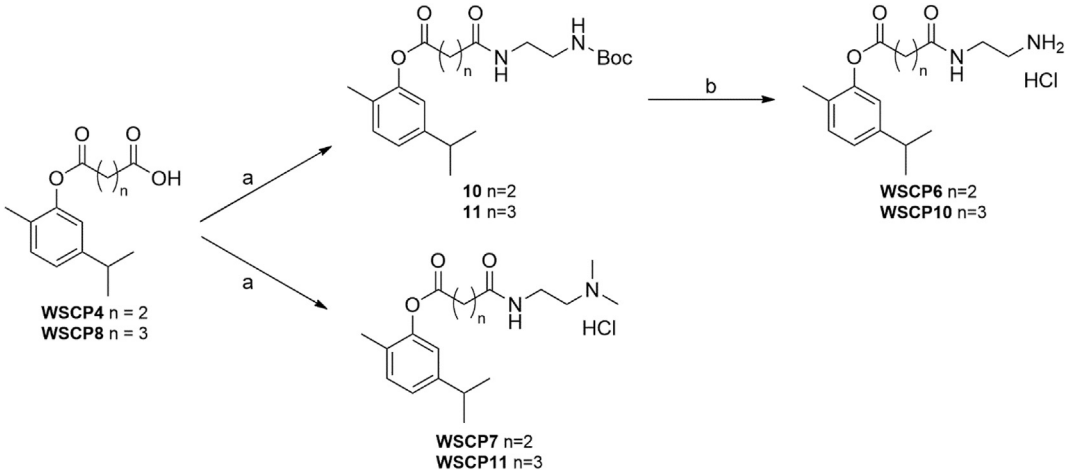

Scheme 3. Synthesis of **WSCP6-7, 10–11**. *Reagents and conditions:* a) Boc-NHCH$_2$CH$_2$NH$_2$ (**10** and **11**) or (CH$_3$)$_2$NCH$_2$CH$_2$NH$_2$ (for the syntheses of **WSCP7** and **WSCP11**), EDC·HCl, TEA, HOBt, dry DMF, rt, 24 h; b) HCl (g), dry EtOAc, 0 °C, 1 h, and rt, 3 h (for the syntheses of **WSCP6** and **WSCP10**).

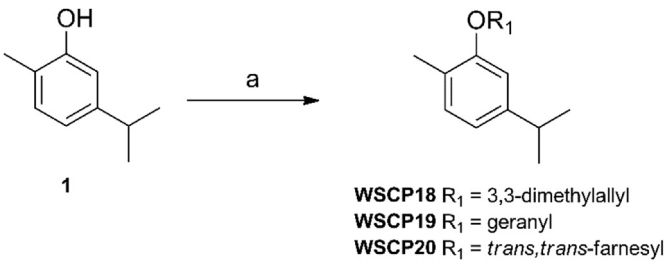

Scheme 4. Synthesis of **WSCP18–20**. *Reagents and conditions*: a) 3,3-Dimethylallylchloride (for the synthesis of **WSCP18**), geranyl chloride (for the synthesis of **WSCP19**) or farnesyl chloride (for the synthesis of **WSCP20**), K_2CO_3, acetone, 80 °C, 2 h.

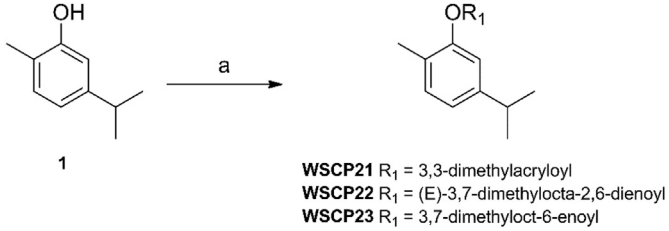

Scheme 5. Synthesis of **WSCP21–23**. *Reagents and conditions:* a) 3,3-Dimethylacryloyl chloride (for the synthesis of **WSCP21**), (2E)-3,7-dimethyl-2,6-octadienoyl chloride (for the synthesis of **WSCP22**), or (R)-citronelloyl chloride (for the synthesis of **WSCP23**), Et_3N, Et_2O, rt, 2–5 h.

experiments. These data suggest that the conjugation of CAR to basic amino acids, such as Lys, Arg, and His, and the introduction of a linker (succinic or glutaric spacer) are not necessary to improve the antimicrobial activity (**WSCP4-17**).

The different antimicrobial activities of **WSCP1-3** and **18–19** could be explained based on the diverse composition of the bacterial cell walls. Teichoic acids, highly abundant in the gram-positive cell walls, are required for many cellular functions and contribute to bacterial cell surface charge and hydrophobicity. The **WSCP18–19** prodrugs, according to their hydrophobic properties (Log P values > 5, Fig. 1) and small size, could easily pass through the cell wall of gram-positive species. The prenylation of the CAR hydroxyl group afforded prodrugs endowed with better membrane permeability and antibacterial properties, suggesting that prenylation correlates with antimicrobial activity, as previously reported [22].

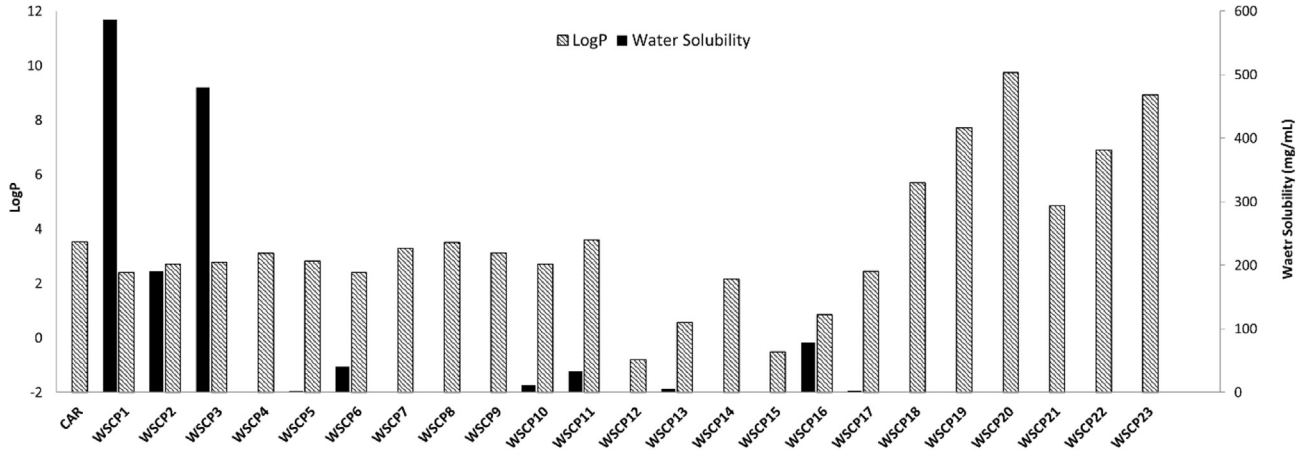

Fig. 1. Chemical-physical properties of **WSCP1-23**.

Table 1
Comparative activities of **WSCP1-3** and **18**–**19**against gram-positive and gram-negative bacteria.

Strain (no.)[a]	MIC (μg/mL)[b]	**WSCP1**	**WSCP2**	**WSCP3**	**WSCP18**	**WSCP19**	CAR
S. aureus	Range	256–512	512	256–512	128–512	64->512	256
(13)	50%	512	512	512	256	256	256
	90%	512	512	512	512	>512	256
S. epidermidis	Range	512->512	512->512	512->512	256–512	256->512	256
(12)	50%	512	512	512	256	>512	256
	90%	512	>512	512	512	>512	256
E. faecalis	Range	256–512	256–512	256–512	64–256	16–512	128–512
(12)	50%	512	512	256	128	64	256
	90%	512	512	512	256	512	256
S. agalactiae	Range	512->512	>512	>512	256–512	512->512	256–512
(11)	50%	>512	>512	>512	256	>512	256
	90%	>512	>512	>512	512	>512	512
S. pyogenes	Range	64–512	128–256	64–512	256–512	512->512	64–256
(10)	50%	128	128	256	512	512	128
	90%	256	256	512	512	>512	256
S. pneumoniae	Range	32–256	64->256	256->256	32–256	16–32	64–256
(11)	50%	256	256	256	64	16	128
	90%	256	>256	>256	64	16	256
E. coli	Range	256–512	512->512	256	>512	>512	256
(12)	50%	256	>512	256	>512	>512	256
	90%	512	>512	256	>512	>512	256
K. pneumoniae	Range	512->512	512->512	512->512	>512	>512	512
(11)	50%	512	512	512	>512	>512	512
	90%	512	>512	>512	>512	>512	512
P. aeruginosa	Range	>512	512->512	512->512	>512	>512	512->512
(11)	50%	>512	512	512	>512	>512	>512
	90%	>512	>512	512	>512	>512	>512
A. baumannii	Range	128–512	64–512	128–512	>512	512->512	64–256
(11)	50%	256	256	128	>512	>512	128
	90%	256	512	256	>512	>512	256

[a] Including ATCC/NCTC reference strains.
[b] 50% and 90%, MICs at which 50% and 90% of isolates are inhibited, respectively.

The cell wall of gram-negative bacteria is more complex [24]. It is composed of a thin layer of peptidoglycan and an outer membrane, formed by a double layer of phospholipids, exposing external porin proteins. Small hydrophilic molecules can pass through the outer membrane via the porin proteins, which function as hydrophilic transmembrane channels [25]. **WSCP1-3** were shown to be effective against some strains of gram-negative bacteria, probably because these prodrugs were hydrophilic, thus allowing them to interact effectively with the porin channels. The positive charge of **WSCP1-3** at physiological pH stabilized the ionic interactions inside the porin channels. In general, the activity against gram-positive or gram-negative bacteria was moderately enhanced with an increase in the lipophilicity or hydrophilicity of the synthetized prodrugs, respectively.

2.4. Inhibition of biofilm formation

Regarding the role of prodrugs in biofilm formation, **WSCP18** and, even more so, **WSCP19**, substantially reduced the biomass of *S. aureus* ATCC 43300 at all assayed concentrations (1/2, 1/4 and 1/8 MIC) (Fig. 2). Notably, **WSCP19** also demonstrated biofilm-inhibiting activity against *S. epidermidis* ATCC 35984, particularly at 1/2 MIC. These data suggest that the prodrugs are involved in the early stages of biofilm formation.

Although several studies have been published, the mechanism of action of CAR on biofilm is still not fully elucidated. However, the antibiofilm activity of CAR has been suggested to depend on its amphipathic nature. In addition to the intrinsic hydrophobic properties – that allow CAR to specifically interact with and

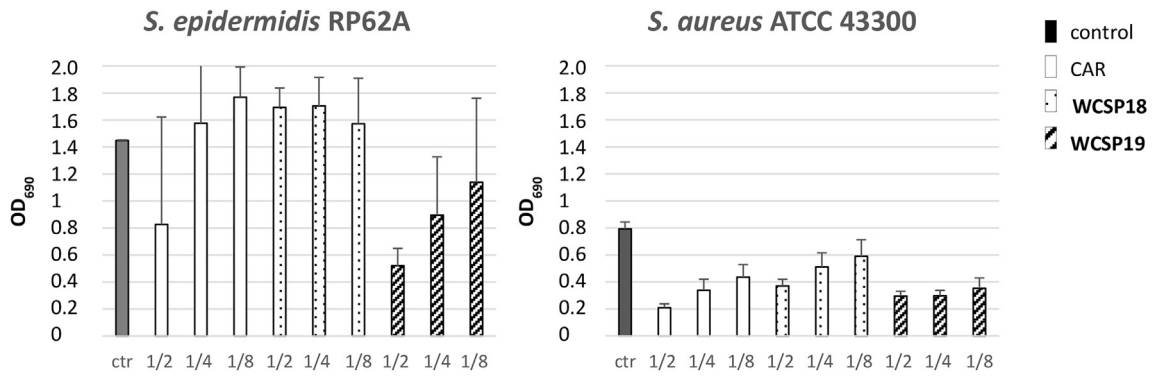

Fig. 2. Biofilm production by ATCC strains in presence of **WSCP18**–**19** at sub-MICs. The values are expressed as the means $OD_{690} \pm$ standard deviations (SD).

consequently damage the lipid bilayer of cytoplasmic membranes – CAR is relatively hydrophilic, which allows it to diffuse through a polar polysaccharide matrix [26]. Because **WSCP18**–**19** showed great hydrophobicity (LogP of 5.69 and 7.72, respectively, Fig. 1), their interaction with the bacterial membrane could be more considerable than that of CAR (LogP 3.5), affecting the protein systems involved in the initial phases of biofilm formation, such as adhesion to the substrate and cell-to-cell communications.

2.5. Scanning electron microscopy (SEM)

SEM-based visualization was performed to analyse the effect of **WSCP18** on *S. aureus* ATCC 43300 biofilms. A significant reduction of the biofilm by ATCC 43300 was related to the increment in **WSCP18** concentrations. The control biofilm exhibited a regular cellular morphology, with clumped cells, and signs that an exopolysaccharide matrix was synthetized (Fig. 3a and b). Conversely, the treated samples showed a reduction in cell density, depending on the increment in drug concentration, with the cells scattered along the surface (Fig. 3c, e, g). Matrix deposition was no longer detected. In addition to observing biofilm dysregulation, we observed alteration of bacterial morphology in the treated cells. The SEM micrographs showed that the cells were dispersed and not clumped, with signs of incomplete septum formation.

2.6. Antifungal activity

The antifungal activity of **WSCP1-23** against different species of fungi is reported in Tables 2 and 3 and expressed as MIC (mg/mL). Isolates of *Candida albicans*, *Candida dubliniensis, Candida parapsilosis, Candida glabrata,* and *Candida tropicalis* have been used to test all prodrugs. **WSCP1** was the most active prodrug against *C. albicans* showing a MIC value equal to 0.8 mg/mL compared to that of fluconazole (MCF = 0.25 mg/mL), a drug of choice for the prevention and treatment of candidiasis (Table 2). Moreover, a disk diffusion assay was performed on several *Candida* species (Table 3), and amphotericin B was used as control. The results showed that the growth of *C. albicans* was inhibited by **WSCP1** and the halo formed was turbid indicating antifungal activity (see Supporting Information). On the other hand, **WSCP3** displayed antifungal properties against *C. tropicalis* and *C. glabrata* when compared to those of amphotericin B. The other compounds did not show any inhibition zone (Supporting Information).

These results confirmed that **WSCP1** and **3**, which showed antimicrobial activity against gram-negative bacteria that was comparable to that of CAR, are endowed with antifungal activity against *C. albicans*, and *C. tropicalis* and *C. glabrata*. The anticandidal properties of CAR were previously studied by Manzoor et al. who demonstrated that monoterpene possessed fungicidal properties, in contrast to the fungistatic activity of fluconazole [27]. The fungicidal mechanism is based on the inhibition of ergosterol biosynthesis and the disruption of membrane integrity. In our study, **WSCP1** and **3** are the most hydrophilic prodrugs and have slightly lower LogP than that of CAR. Balancing the hydrophilic and hydrophobic features of these compounds could help them dissolve in the microbial membrane and impair ergosterol biosynthesis, which is significant for the integrity of the fungal membrane.

2.7. Haemolytic activity

The *in vitro* haemolytic activity of **WSCPs** against human erythrocytes was determined using prodrug concentrations ranging from 0.1 to 500 μM (Supporting Information). Each concentration shows the mean of haemolysis percentage of three repetitions. The induced haemolysis rates of **WSCPs** in red blood cells were concentration dependent, but all prodrugs showed slight haemolytic activity against human erythrocytes at concentrations lower than 250 μM. At higher concentrations, the observed haemolytic levels were elevated compared to the control value at $p < 0.05$ (see Supporting Information).

2.8. Cytotoxic activity

The cytotoxic activity of the most promising derivatives **WSCP1-3** and **18**–**19** towards HaCaT cells (human skin keratinocytes) was determined by the MTT assay (Supporting Information). Compared to control^{-} cells, all tested prodrugs did not exhibit cytotoxic activities at concentrations lower than 50 μM. Furthermore, **WSCP3** was found to be non-cytotoxic at all tested concentrations. However, the relatively higher concentrations of **WSCP1** (50 and 100 μM), **WSCP2** (100 μM), **WSCP18** (50 and 100 μM), and **WSCP19** (50 and 100 μM) executed cytotoxic action against the HaCaT cells. Cell viability analysis revealed that the tested prodrugs at concentrations ≤50 μM are safe since they do not induce cytotoxic damage in cultured HaCaT cells. Therefore, the exposure to our prodrugs did not impair the proliferation and viability of keratinocytes.

2.9. Stability studies

The most active prodrugs (**WSCP1-3** and **18**–**19**) were subjected to stability studies in simulated fluids and human plasma (Figs. 4–5). Prodrug stability was evaluated in the presence of pepsin (3.2 mg/mL) and pancreatin (10 mg/mL) for 1 h and 3 h, respectively. The relative difference (*RD)* between the amount of

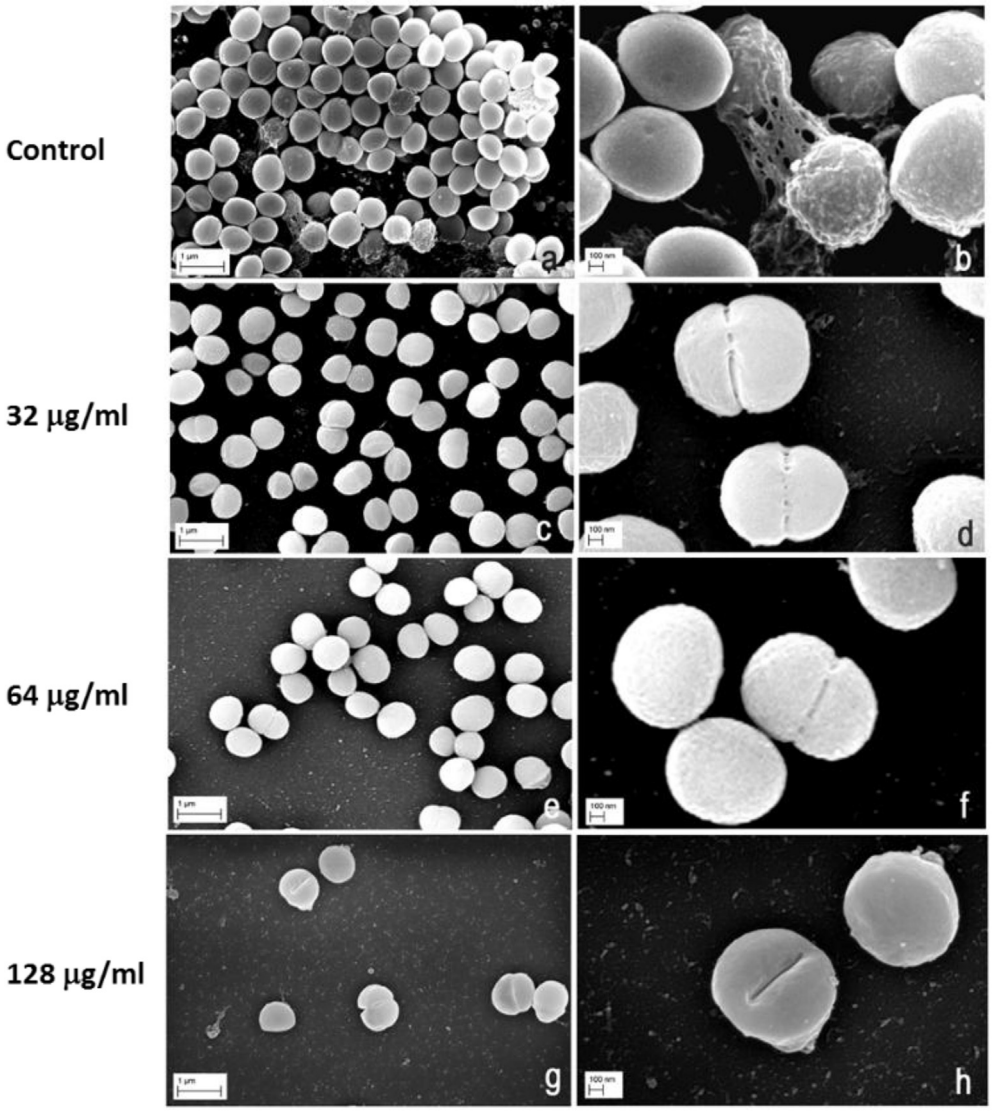

Fig. 3. SEM images of the *S. aureus* ATCC 43300 biofilm. a) Control biofilm showing high density, cell cluster and polysaccharide material; b) High magnification image of the same field focusing on the matrix deposition among cells (evidence of fibrillar meshwork-like structures between cells); c, e, g) Biofilm after treatment with **WSCP18**, showing that cell density was reduced with the increment in drug concentration. Matrix deposition was no longer detected; d, f, h). High magnification image of the respective samples showing morphological details indicating anomalous division septum.

Table 2
Antifungal activities of **WSCP 1**–**23**[a].

Compd	*C. albicans*
Flucanozole	0.25
CAR	1.25
WSCP 1	0.8
WSCP 2	2.5
WSCP 5	6.4
WSCP 6	3.2 mg/mL
WSCP 3–**4, 7-23**	> 6.4 mg/mL

[a] MIC value expressed as mg/mL.

drug added and that determined at the end of the incubation period was calculated as reported in the formula, where *Ci* is the amount of drug found at the zero time point and Cf is the amount found at the end of incubation. The *RD* value gives a measure of the extent of degradation of any drug in the presence of gastrointestinal fluids. An *RD* value > 5% indicates s significant degradation of the drug [28].

$$RD = (C_i - C_f)/C_i$$

The results showed that **WSCP1-3** and **19** were quite stable in the simulated gastric fluid (SGF, pH 1.2) for 1 h incubation period, in contrast to **WSCP18** (*RD* > 15% after 30 min). Exposure of the prodrugs at 37 °C to simulated intestinal fluids (SIF, pH 6.8) revealed that **WSCP18**–**19** were the most stable up to 3 h while **WSCP1-3** were rapidly degraded, suggesting a potential instability in the intestinal tract (Fig. 4). These data could be explained on the basis of the structure of **WSCP1-3**, which contains an ester linkage liable to a basic environment, while **WSCP18**–**19** present an ether bond more resistant to alkaline hydrolysis. In human plasma, **WSCP1-3** were rapidly hydrolysed while **WSCP18**–**19** showed a longer half-life ($t_{1/2}$ = 23.5 and 4 h, respectively) confirming that plasma enzymes accelerate the degradation of prodrugs (Fig. 5). Enzymes,

Table 3
Inhibition zone of **WSCP1-3** (millimetres).

compd	*C. albicans*	*C. tropicalis*	*C. parapsilosis*	*C. glabrata*	*C. dubliniensis*
WSCP1	14	8	–	9	9
WSCP2	9	8	7	9	12
WSCP3	–	12	7	12	–
CAR	9	10	7	8	7
Amphotericin B	10	10	9	12	10

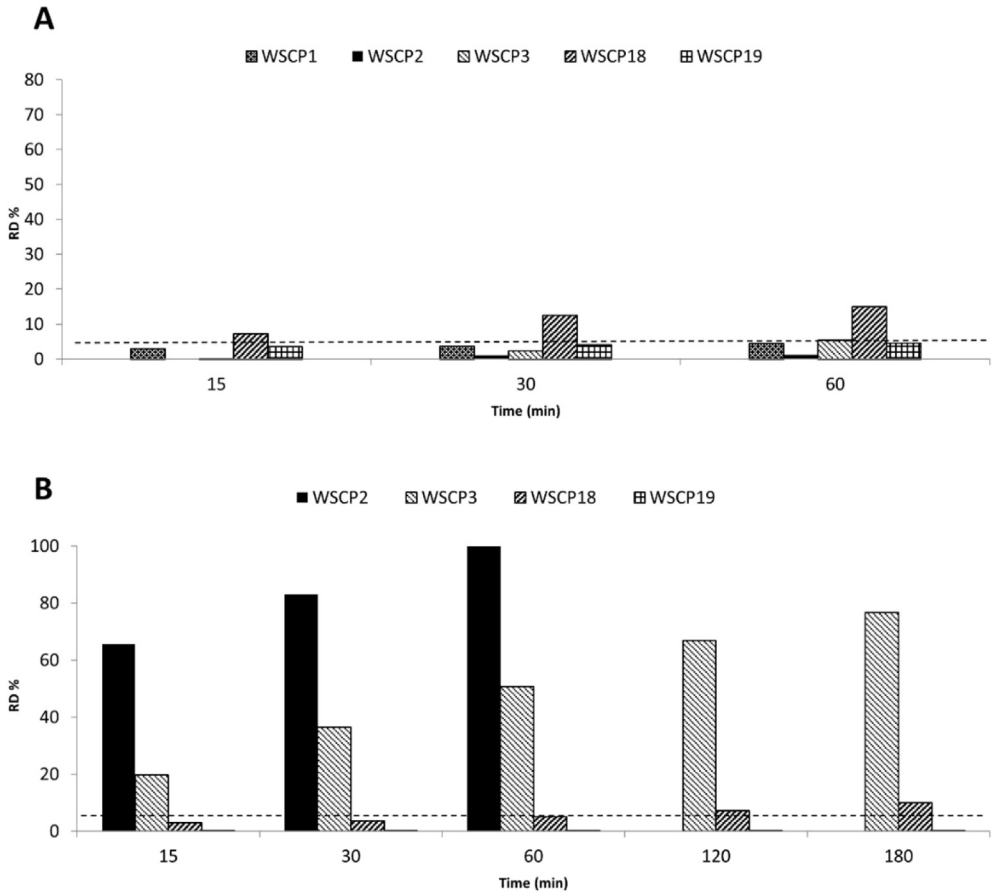

Fig. 4. Stability studies in A) SGF (pH 1.2, pepsin 3.2 mg/mL) and B) SIF (pH 6.8, pancreatin 10 mg/mL).

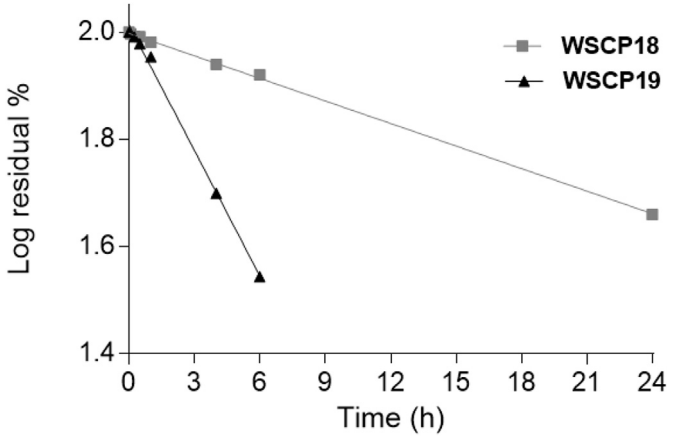

Fig. 5. Human plasma stability profiles of **WSCP18**–**19**.

such as esterases, amidases, and/or peptidases, in plasma or in other tissues can bio-convert **WSCPs** to their active single constituents. The amino acid esters or amides in **WSCP1-17** were used as ionizable groups and introduced into the hydroxyl group of the parent compound to enhance water solubility. In this context, these moieties could also be used to enhance the absorption and consequently oral drug delivery of the parent drug, because the brush-border membrane of intestinal epithelium possesses a considerable number of transporters for amino acids and peptides [29].

All data showed that **WSCP18**–**19** possessed good stability in simulated fluids and plasma and were the best candidates for the treatment of infections caused by gram-positive bacteria. Notably, **WSCP18**–**19** can interfere with the biofilm production of *S. aureus* and *epidermidis* in the early stages of biofilm formation. However, as they are not water-soluble prodrugs, they may reach higher concentrations in tissues than in plasma suggesting a potential investigation in skin infections.

On the other hand, **WSCP1-3** were water-soluble prodrugs, but they underwent rapid hydrolysis in simulated fluids and human

plasma, suggesting that they are not suitable for oral administration. These prodrugs, possessing antimicrobial profile comparable to that of CAR and a lack of toxicity towards HaCaT cells, showed antifungal properties against different species of *Candida* and could be considered for further studies in the treatment of candidiasis.

Further experiments will be performed in animal experimental models to investigate the pharmacological potential of the synthetized prodrugs and evaluate their *in vivo* efficacy and pharmacokinetic profiles.

3. Experimental section

3.1. Materials and methods

All reagents, unless otherwise stated, were provided by Sigma-Aldrich Co (St. Louis, MO, USA). Chromatographic columns were performed on silica gel using column chromatography (Merck 60, 230–400 mesh ASTM silica gel), and co. Melting points were determined on Stuart melting point SMP30 apparatus. NMR spectra were recorded with a Varian VXR-300 spectrometer (Varian Medical Systems, Inc., Palo Alto, CA, USA). Mass spectra were obtained by electrospray ionization (ESI) in positive mode using LCQ (Thermo Finnigan) ion trap mass spectrometer (San Jose, CA, USA) equipped with an electrospray ionization (ESI) source. Analyses indicated by the symbols of the elements or functions were within ±0.4% of the theoretical values. Purity and chemical structures of compounds **WSCP1-23** were confirmed by HPLC and ^{1}H,^{13}C NMR, and MS spectra data, respectively.

3.1.1. Synthesis of WSCP1-3

Boc-protected amino acid (5.7 mmol) was dissolved in dry DCM (27 mL) prior to the addition of DCC (5.71 mmol) and stirred for 1 h at room temperature. Then, CAR (5.71 mmol) and a catalytic amount of DMAP (0.19 mmol) were added and the mixture was left under stirring for 24 h at room temperature. After evaporating the solvent, the crude residue was extracted with EtOAc and brine. Chromatographic purification was performed using DCM as eluent to provide the *N*-Boc-protected intermediates in good yields.

To remove the Boc-protection, an ice bath solution of the suitable Boc-protected precursor (2.43 mmol) in dry EtOAc (13 mL) was saturated with HCl (g) for 10 min and then left for 1 h at room temperature under stirring. After evaporation of the solvent, **WSCP1-3** were obtained as white pure solid.

3.1.2. 5-Isopropyl-2-methylphenyl-2-aminoacetate hydrochloride (WSCP1)

MP: 73–75 °C. Yield: qtt; $R_f = 0.08$, DCM; ^{1}H NMR (300 MHz, $CDCl_3$) δ: 1.14 (6H, d, $J = 6.9$ Hz), 2.02 (3H, s), 2.74–2.82 (1H, m), 4.06 (2H, s), 6.92 (1H, s), 6.95 (1H, d, $J = 9.6$ Hz), 7.03 (1H, d, $J = 7.5$ Hz), 8.75 (3H, br s); ^{13}C NMR (75 MHz, $CDCl_3$) δ: 15.9, 23.9 (2 x CH_3), 33.5, 40.5, 119.7, 124.4, 127.1, 130.9, 148.1, 148.5, 166.2. Anal. Calcd for $C_{12}H_{18}ClNO_2$: C, 59.13; H, 7.44; Cl, 14.55; N, 5.75; O, 13.13. Found: C, 59,11; H, 7.39; Cl, 14.50, N, 5.71; O, 13.19. MS (ESI, *m*/*z*): 266.72 $[M+H]^+$.

3.1.3. (R)-5-Isopropyl-2-methylphenyl-2-aminopropanoate hydrochloride (WSCP2)

MP: 153–154 °C. Yield: qtt; $R_f = 0.10$, DCM; ^{1}H NMR (300 MHz, $CDCl_3$) δ: 1.17 (6H, d, $J = 7.2$ Hz), 1.71 (3H, d, $J = 6.6$ Hz), 2.07 (3H, s), 2.76–2.83 (1H, m), 4.40 (1H, br s), 6.95 (1H, s), 6.98 (1H, d, $J = 8.1$ Hz), 7.07 (1H, d, $J = 7.5$ Hz), 8.84 (3H, br s); ^{13}C NMR (75 MHz, $CDCl_3$) δ: 15.9, 23.8, 24.0 (2 x CH_3), 33.5, 49.5, 119.8, 124.4, 127.1, 130.9, 148.1, 148.6, 168.7. Anal. Calcd for $C_{13}H_{20}ClNO_2$: C, 60.58; H, 7.82; Cl, 13.75; N, 5.43; O, 12.41. Found: C, 60.50; H, 7.83; Cl, 13.79; N, 5.39; O, 12.48. MS (ESI, *m*/*z*): 280.75 $[M+Na]^+$.

3.1.4. 5-Isopropyl-2-methylphenyl-3-aminopropanoate hydrochloride (WSCP3)

MP: 72–73 °C. Yield: qtt; $R_f = 0.06$, DCM; ^{1}H NMR (300 MHz, $CDCl_3$) δ: 1.19 (6H, d, $J = 6.9$ Hz), 2.10 (3H, s), 2.81–2.87 (1H, m), 3.06 (2H, t, $J = 6.3$ Hz), 3.26–3.29 (2H, m), 6.93 (1H, s), 6.98 (1H, d, $J = 7.5$ Hz), 7.09 (1H, d, $J = 8.1$ Hz), 8.27 (3H, br s); ^{13}C NMR (75 MHz, $CDCl_3$) δ: 15.9, 23.9 (2 x CH_3), 31.1, 33.5, 35.3, 119.8, 124.4, 127.1, 130.9, 148.2, 148.8, 169.8. Anal. Calcd for $C_{13}H_{20}ClNO_2$: C, 60.58; H, 7.82; Cl, 13.75; N, 5.43; O, 12.41. Found: C, 60.60; H, 7.80; Cl, 13.77; N, 5.40; O, 12.44. MS (ESI, *m*/*z*): 280.75 $[M+Na]^+$.

3.1.5. Synthesis of WSCP4 and WSCP8

A solution of **1** (1.4 mL, 9.08 mmol) in dry THF/Et_2O (1:2) was added with the proper anhydride (succinic for **WSCP4** or glutaric for **WSCP8**) (9.99 mmol) and DCHA (1.98 mL, 9.99 mmol). The mixture was stirred for 24 h at room temperature, then filtered and dried under vacuum. After silica gel column chromatography with $CHCl_3$/MeOH (95:5) as eluent, the final compounds (**WSCP4** and **WSCP8**) were obtained as oils in discrete yields.

3.1.6. 4-(5-Isopropyl-2-methylphenoxy)-4-oxobutanoic acid (WSCP4)

Yield: 32%; $R_f = 0.65$, $CHCl_3$/MeOH (95:5); ^{1}H NMR (300 MHz, $CDCl_3$) δ: 1.26 (6H, d, $J = 7.2$ Hz), 2.16 (3H, s), 2.81–2.88 (2H, m), 2.90–2.94 (3H, m, CH_2 and CH), 6.89 (1H, s), 7.05 (1H, d, $J = 7.2$ Hz), 7.17 (1H, d, $J = 8.4$ Hz); ^{13}C NMR (75 MHz, $CDCl_3$) δ: 15.7, 23.9 (2 x CH_3), 28.8, 29.0, 33.6, 119.7, 124.3, 127.2, 131.0, 148.1, 149.1, 170.6, 178.6. Anal. Calcd for $C_{14}H_{18}O_4$: C, 67.18; H, 7.25; O, 25.57. Found: C, 67.20; H, 7.23; O, 25.56. MS (ESI, *m*/*z*): 251.4 $[M+H]^+$.

3.1.7. 5-(5-Isopropyl-2-methylphenoxy)-5-oxopentanoic acid (WSCP8)

Yield: 65%; $R_f = 0.71$, $CHCl_3$/MeOH (95:5); ^{1}H NMR (300 MHz, DMSO-d_6) δ: 1.14 (6H, d, $J = 6.9$ Hz), 1.84 (2H, m), 2.02 (3H, s), 2.32 (2H, t, $J = 7.8$ Hz), 2.62 (2H, t, $J = 7.2$ Hz), 2.80–2.85 (1H, m), 6.89 (1H, s), 7.01 (1H, d, $J = 9.3$ Hz), 7.16 (1H, d, $J = 8.1$ Hz); ^{13}C NMR (75 MHz, DMSO-d_6) δ: 15.8, 20.4, 24.2 (2 x CH_3), 32.9, 33.1, 33.3, 120.2, 124.3, 127.3, 131.1, 148.1, 149.5, 171.6, 174.4. Anal. Calcd for $C_{15}H_{20}O_4$: C, 68.16; H, 7.63; O, 24.21. Found: C, 68.20; H, 7.58; O, 24.23. MS (ESI, *m*/*z*): 265.84 $[M+H]^+$.

3.1.8. General coupling procedure for compounds 2–9

A solution of **WSCP4** (for **2**, **4**–**6**) or **WSCP8** (for **3**, **7**–**9**) (1.79 mmol), TEA (0.24 mL, 1.72 mmol), and IBCF (0.24 mL, 1.79 mmol) in dry DMF (6 mL) was stirred for 20 min at −15 °C. Afterwards, a solution of the suitable amino acid (1.72 mmol) and TEA (0.24 mL, 1.79 mmol) in dry DMF (4 mL) was dropped into the reaction mixture and stirred for further 3 h at 0 °C, then 15 h at room temperature. After filtration and evaporation of the solvent, the crude product was purified on silica gel with DCM/EtOAc (8:2) (**2**), $CHCl_3$/MeOH (95:5) (**3**), Cyclohexane/EtOAc (1:1) (**4**–**9**) as eluent systems to provide compounds **2**–**9** in good yields.

3.1.9. 5-Isopropyl-2-methylphenyl-4-((2-(tert-butoxy)-2-oxoethyl) amino)-4-oxobutanoate (2)

Yield: 36%; $R_f = 0.59$, DCM/EtOAc (8:2); ^{1}H NMR (300 MHz, $CDCl_3$) δ: 1.21 (6H, d, $J = 7.2$ Hz), 1.45 (9H, s), 2.11 (3H, s), 2.64 (2H, t, $J = 6.3$ Hz), 2.81–2.87 (1H, m), 2.94 (2H, t, $J = 6.6$ Hz), 3.92 (2H, d, $J = 5.4$ Hz), 6.25 (1H, br s), 6.86 (1H, s), 6.99 (1H, d, $J = 8.1$ Hz), 7.11 (1H, d, $J = 7.5$ Hz); ^{13}C NMR (75 MHz, $CDCl_3$) δ: 15.7, 23.9 (2 x CH_3), 28.0, 29.3, 30.6, 33.5, 42.1, 82.2, 119.7, 124.1, 127.2, 130.8, 148.0, 149.2, 169.0, 171.1, 171.3.

3.1.10. 5-Isopropyl-2-methylphenyl-5-((2-(tert-butoxy)-2-oxoethyl)amino)-5-oxopentanoate (3)

Yield: 65%; $R_f = 0.74$, $CHCl_3$/MeOH (95:5); ^{1}H NMR (300 MHz, $CDCl_3$) δ: 1.21 (6H, d, $J = 7.2$ Hz), 1.46 (9H, s), 2.07–2.15 (5H, m, CH_3 and CH_2), 2.39 (2H, t, $J = 7.5$ Hz), 2.67 (2H, t, $J = 6.9$ Hz), 2.82–2.88 (1H, m), 3.93 (2H, d, $J = 5.1$ Hz), 6.08 (1H, br s), 6.84 (1H, s), 6.99 (1H, d, $J = 8.4$ Hz), 7.12 (1H, d, $J = 8.4$ Hz); ^{13}C NMR (75 MHz, $CDCl_3$) δ: 15.7, 20.8, 23.8, 28.1, 32.9, 33.5, 34.7, 41.6, 119.6, 124.6, 127.0, 131.1, 148.3, 148.9, 169.1, 172.5, 173.1.

3.1.11. (S)-Tert-butyl-5-guanidino-2-(4-(5-isopropyl-2-methylphenoxy)-4-oxobutanamido)pentanoate (4)

Yield: 54%; $R_f = 0.28$, Cyclohexane/EtOAc (1:1); ^{1}H NMR (300 MHz, $CDCl_3$) δ: 1.20 (6H, d, $J = 7.2$ Hz), 1.43 (2H, s), 1.45 (9H, s), 1.78 (2H, m), 1.82 (3H, s), 2.08 (2H, s), 2.66 (1H, br s), 2.75–2.83 (1H, m), 3.02–3.21 (6H, m, 3 x CH_2), 3.91 (1H, s), 6.75 (1H, m), 7.04 (1H, m), 7.16 (1H, m), 7.79 (1H, m); ^{13}C NMR (75 MHz, $CDCl_3$) δ: 15.4, 23.9 (2 x CH_3), 25.2, 27.5, 28.1, 29.2, 30.4, 33.4, 41.7, 51.9, 82.1, 119.6, 123.9, 127.2, 130.6, 147.9, 149.5, 161.3, 171.9, 172.2, 173.5.

3.1.12. (S)-Benzyl-6-(benzylamino)-2-(4-(5-isopropyl-2-methylphenoxy)-4-oxobutanamido)hexanoate (5)

Yield: 33%; $R_f = 0.93$, Cyclohexane/EtOAc (1:1); ^{1}H NMR (300 MHz, $CDCl_3$) δ: 1.20 (6H, d, $J = 6.6$ Hz), 1.32–1.43 (3H, m, CH_2 and CH), 1.59–1.73 (2H, m), 1.79–1.88 (2H, m), 2.09 (3H, s), 2.62 (2H, t, $J = 6.6$ Hz), 2.82–3.08 (4H, m, 2 x CH_2), 4.62–4.68 (1H, m), 4.90 (1H, br s), 5.07 (2H, s), 5.20 (2H, m), 6.45 (1H, d, $J = 8.1$ Hz), 6.85 (1H, s), 6.99 (1H, d, $J = 8.1$ Hz), 7.10 (1H, d, $J = 7.5$ Hz), 7.31 (10H, br s); ^{13}C NMR (75 MHz, $CDCl_3$) δ: 15.8, 22.0, 23.9 (2 x CH_3), 26.9, 29.3, 30.6, 31.8, 33.5, 40.3, 52.1, 66.5, 67.2, 119.7, 124.4, 127.2, 128.1 (2 x CH), 128.4 (2 x CH), 128.5 (2 x CH), 128.6 (2 x CH), 128.7 (2 x CH), 130.9, 135.3, 136.6, 148.0, 149.2, 156.6, 171.1, 171.3, 172.2.

3.1.13. (S)-5-Isopropyl-2-methylphenyl-4-((1-(benzyloxy)-3-(1H-imidazol-5-yl)-1-oxopropan-2-yl)amino)-4-oxobutanoate (6)

Yield: 42%; $R_f = 0.92$, Cyclohexane/EtOAc (1:1); ^{1}H NMR (300 MHz, $CDCl_3$) δ: 1.21 (6H, d, $J = 6.6$ Hz), 2.01–2.08 (1H, m), 2.10 (3H, s), 2.69–2.95 (6H, m, 3 x CH_2), 4.02 (1H, t, $J = 7.1$ Hz), 5.12 (1H, m), 5.18 (2H, s), 6.81–6.89 (1H, m), 6.93 (1H, m), 6.99–7.04 (2H, m), 7.11–7.17 (2H, m), 7.32–7.40 (5H, m); ^{13}C NMR (75 MHz, $CDCl_3$) δ: 15.6, 23.7 (2 x CH_3), 28.8, 29.2, 29.9, 33.4, 57.2, 66.4, 118.6, 119.6, 124.3, 127.1, 128.2, 128.3, 128.4, 128.5, 128.6, 130.7, 135.6, 136.2, 137.1, 148.1, 149.3, 171.2, 171.4, 172.9.

3.1.14. (S)-Tert-butyl-5-guanidino-2-(5-(5-isopropyl-2-methylphenoxy)-5-oxopentanamido)pentanoate (7)

Yield: 39%; $R_f = 0.95$, Cyclohexane/EtOAc (1:1); ^{1}H NMR (300 MHz, CD_3OD) δ: 1.21 (6H, d, $J = 7.2$ Hz), 1.42 (9H, s), 1.62–1.99 (6H, m, 3 x CH_2), 2.0–2.08 (1H, m), 2.11 (3H, s), 2.40 (2H, t, $J = 6.6$ Hz), 2.67 (2H, t, $J = 6.7$ Hz), 3.31–3.37 (2H, m), 4.22–4.30 (1H, m), 6.84 (1H, s), 7.01 (1H, d, $J = 8.4$ Hz), 7.17 (1H, d, $J = 8.1$ Hz); ^{13}C NMR (75 MHz, CD_3OD) δ: 14.6, 20.8, 22.9 (2 x CH_3), 25.0, 28.2, 28.5, 32.5, 33.4, 34.2, 40.3, 51.9, 75.3, 119.5, 123.6, 127.0, 130.5, 147.9, 149.6, 157.3, 170.1, 173.8, 175.5.

3.1.15. (S)-Benzyl-6-(benzylamino)-2-(5-(5-isopropyl-2-methylphenoxy)-5-oxopentanamido)hexanoate (8)

Yield: 65%; $R_f = 0.85$, Cyclohexane/EtOAc (1:1); ^{1}H NMR (300 MHz, $CDCl_3$) δ: 1.22 (6H, d, $J = 6.6$ Hz), 1.31–1.40 (2H, m), 1.61–1.72 (2H, m), 1.77–1.88 (2H, m), 1.89–1.93 (2H, m), 1.95–2.02 (1H, m), 2.10 (3H, s), 2.61 (2H, t, $J = 6.7$ Hz), 2.80–3.05 (4H, m, 2 x CH_2), 4.61–4.66 (1H, m), 4.91 (1H, br s), 5.09 (2H, s), 5.22 (2H, m), 6.46 (1H, d, $J = 8.2$ Hz), 6.84 (1H, s), 7.00 (1H, d, $J = 8.0$ Hz), 7.11 (1H, d, $J = 7.4$ Hz), 7.30 (10H, br s); ^{13}C NMR (75 MHz, $CDCl_3$) δ: 15.7, 22.1, 23.8 (2 x CH_3), 25.8, 26.7, 29.1, 30.4, 31.6, 33.4, 40.2, 52.0, 66.4, 67.1, 119.8, 124.3, 127.2, 128.0 (2 x CH), 128.3 (2 x CH), 128.4 (2 x CH), 128.5 (2 x CH), 128.6 (2 x CH), 130.7, 135.1, 136.4, 148.1, 149.0, 156.5, 171.0, 171.4, 172.3.

3.1.16. (S)-5-Isopropyl-2-methylphenyl-5-((1-(benzyloxy)-3-(1H-imidazol-4-yl)-1-oxopropan-2-yl)amino)-5-oxopentanoate (9)

Yield: 81%; $R_f = 0.57$, Cyclohexane/EtOAc (1:1); ^{1}H NMR (300 MHz, $CDCl_3$) δ: 1.20 (6H, d, $J = 6.6$ Hz), 1.61–1.84 (2H, m), 2.07 (3H, s), 2.37 (2H, t, $J = 7.5$ Hz), 2.61 (2H, t, $J = 7.7$ Hz), 2.80–2.89 (1H, m), 3.04–3.17 (2H, m), 4.55–4.62 (1H, m), 5.06 (2H, s), 6.22 (1H, d, $J = 6.5$ Hz), 6.83 (1H, s), 6.99 (1H, d, $J = 8.4$ Hz), 7.09 (1H, d, $J = 8.2$ Hz), 7.27–7.35 (8H, m, 7 x CH Ar and 1 NH); ^{13}C NMR (75 MHz, $CDCl_3$) δ: 15.4, 23.5 (2 x CH_3), 28.6, 28.9, 29.1, 30.0, 33.5, 57.1, 66.3, 118.9, 119.8, 124.2, 127.0, 128.0, 128.2, 128.4, 128.5, 128.7, 130.4, 135.5, 136.1, 137.0, 148.2, 149.1, 171.1, 171.3, 172.8.

3.1.17. ***Synthesis of WSCP5, WSCP9, WSCP12,*** *and* ***WSCP15***

A suitable *tert*-butyl ester (**2**–**4** and **7**) (0.96 mmol) was dissolved in a large excess of TFA (1.56 mL, 20.37 mmol) and stirred for 3 h at room temperature. The solvent was then removed under vacuum to quantitatively give the final pure compounds as oils.

3.1.18. 2-(4-(5-Isopropyl-2-methylphenoxy)-4-oxobutanamido) acetic acid (WSCP5)

Yield: qtt; $R_f = 0.31$, DCM/EtOAc (8:2); ^{1}H NMR (300 MHz, $CDCl_3$) δ: 1.22 (6H, d, $J = 6.9$ Hz), 2.10 (3H, s), 2.64 (2H, t, $J = 6.3$ Hz), 2.85–2.92 (3H, m, CH and CH_2), 3.98 (2H, d, $J = 5.1$ Hz), 6.87 (1H, s), 7.03 (1H, d, $J = 7.5$ Hz), 7.13 (1H, d, $J = 8.1$ Hz), 9.60 (1H, br s); ^{13}C NMR (75 MHz, $CDCl_3$) δ: 15.6, 23.8 (2 x CH_3), 29.2, 30.1, 33.5, 41.4, 119.6, 124.4, 127.2, 131.0, 148.2, 149.1, 171.9, 172.8, 173.6. Anal. Calcd for $C_{16}H_{21}NO_5$: C, 62.53; H, 6.89; N, 4.56; O, 26.03. Found: C, 62.60; H, 6.84; N, 4.50; O, 26.05. MS (ESI, *m*/*z*): 308.16 $[M+H]^+$.

3.1.19. 2-(5-(5-Isopropyl-2-methylphenoxy)-5-oxopentanamido) acetic acid (WSCP9)

Yield: qtt; $R_f = 0.41$, $CHCl_3$/MeOH (95:5); ^{1}H NMR (300 MHz, $CDCl_3$) δ: 1.20 (6H, d, $J = 7.2$ Hz), 2.01–2.11 (5H, m, CH_3 and CH_2), 2.42 (2H, t, $J = 7.5$ Hz), 2.68 (2H, t, $J = 6.9$ Hz), 2.81–2.89 (1H, m), 4.02 (2H, d, $J = 5.1$ Hz), 6.81 (1H, s), 6.92 (1H, br s), 7.01 (1H, d, $J = 8.4$ Hz), 7.13 (1H, d, $J = 8.4$ Hz), 10.22 (1H, br s); ^{13}C NMR (75 MHz, $CDCl_3$) δ: 15.7, 20.9, 23.8 (2 x CH_3), 32.8, 33.5, 34.7, 41.4, 119.5, 124.5, 126.9, 131.0, 148.3, 148.9, 172.5, 173.1, 175.1. Anal. Calcd for $C_{17}H_{23}NO_5$: C, 63.54; H, 7.21; N, 4.36; O, 24.89. Found: C, 63.56; H, 7.18; N, 4.32; O, 24.93. MS (ESI, *m*/*z*): 360.0 $[M+K]^+$.

3.1.20. (S)-5-Guanidino-2-(4-(5-isopropyl-2-methylphenoxy)-4-oxobutanamido)pentanoic acid (WSCP12)

Yield: qtt; $R_f = 0.1$, Cyclohexane/EtOAc (1:1); ^{1}H NMR (300 MHz, CD_3OD) δ: 1.21 (6H, d, $J = 7.1$ Hz), 1.62–1.79 (4H, m, 2 x CH_2), 1.85–2.01 (1H, m), 2.09 (3H, s), 2.65–3.00 (6H, m, 3 x CH_2), 4.43 (1H, m), 6.84 (1H, s), 7.01 (1H, d, $J = 7.5$ Hz), 7.15 (1H, d, $J = 8.1$ Hz); ^{13}C NMR (75 MHz, CD_3OD) δ: 15.4, 23.8 (2 x CH_3), 25.1, 27.4, 28.2, 29.4, 33.5, 41.6, 52.5, 119.7, 123.9, 127.1, 130.5, 147.9, 149.4, 161.4, 171.8, 172.5, 173.6. Anal. Calcd for $C_{20}H_{30}N_4O_5$: C, 59.10; H, 7.44; N, 13.78; O, 19.68. Found: C, 59.15; H, 7.40; N, 13.81; O, 19.65. MS (ESI, *m*/*z*): 429.71 $[M+Na]^+$.

3.1.21. (S)-5-Guanidino-2-(5-(5-isopropyl-2-methylphenoxy)-5-oxopentanamido)pentanoic acid (WSCP15)

Yield: qtt; $R_f = 0.28$, Cyclohexane/EtOAc (1:1); ^{1}H NMR (300 MHz, CD_3OD) δ: 1.21 (6H, d, $J = 7.2$ Hz), 1.61–2.04 (6H, m, 3 x CH_2), 2.09 (3H, s), 2.41 (2H, t, $J = 6.6$ Hz), 2.66 (2H, t, $J = 6.7$ Hz), 2.81–2.89 (1H, m), 3.11–3.22 (2H, m), 4.38–4.42 (1H, m), 6.83 (1H, s), 7.00 (1H, d, $J = 8.4$ Hz), 7.16 (1H, d, $J = 8.1$ Hz); ^{13}C NMR (75 MHz, CD_3OD) δ: 14.5, 20.7, 22.9 (2 x CH_3), 25.0, 28.5, 32.6, 33.4, 34.2, 40.5,

52.0, 119.4, 123.7, 127.0, 130.4, 148.0, 149.6, 157.2, 171.8, 173.9, 175.7. Anal. Calcd for $C_{21}H_{32}N_4O_5$: C, 59.98; H, 7.67; N, 13.32; O, 19.02. Found: C, 59.99; H, 7.63; N, 13.37; O, 19.02. MS (ESI, *m*/*z*): 421.87 $[M+H]^+$.

3.1.22. *Synthesis of WSCP13–14 and WSCP16–17*

The benzyloxy-protected compounds (**5**, **6**, **8**, and **9**) (0.4 mmol) were solubilized in dry MeOH (10 mL). Catalytic amounts of AcOH (0.24 mL) and Pd/C (30%) were added and the mixture was stirred for 6 h at room temperature under hydrogen atmosphere. The catalyst was removed by filtration and the solvent dried under vacuum to provide the final pure compounds as oils.

3.1.23. *(S)-6-Amino-2-(4-(5-isopropyl-2-methylphenoxy)-4-oxobutanamido)hexanoic acid (WSCP13)*

Yield: 87%; $R_f = 0.12$, Cyclohexane/EtOAc (1:1); ^{1}H NMR (300 MHz, CD_3OD) δ: 1.21 (6H, d, $J = 7.2$ Hz), 1.41–1.49 (2H, m), 1.62–1.74 (4H, m, 2 x CH_2), 1.84–1.89 (1H, m), 2.10 (3H, s), 2.65–2.71 (2H, m), 2.80–2.95 (4H, m, 2 x CH_2), 4.34–4.37 (1H, m), 6.87 (1H, s), 7.01 (1H, d, $J = 8.1$ Hz), 7.14 (1H, d, $J = 7.5$ Hz); ^{13}C NMR (75 MHz, CD_3OD) δ: 14.5, 22.2, 22.9 (2 x CH_3), 26.6, 28.7, 29.7, 31.1, 33.4, 39.1, 52.5, 119.4, 123.7, 127.1, 130.4, 147.9, 149.1, 171.6, 171.8, 172.5. Anal. Calcd for $C_{20}H_{30}N_2O_5$: C, 63.47; H, 7.99; N, 7.40; O, 21.14. Found: C, 63.53; H, 8.01; N, 7.42; O, 21.14. MS (ESI, *m*/*z*): 379.67 $[M+H]^+$.

3.1.24. *(S)-3-(1H-Imidazol-4-yl)-2-(4-(5-isopropyl-2-methylphenoxy)-4-oxobutanamido)propanoic acid (WSCP14)*

Yield: 48%; $R_f = 0.11$, Cyclohexane/EtOAc (1:1); ^{1}H NMR (300 MHz, DMSO-d_6) δ: 1.19 (6H, d, $J = 7.2$ Hz), 1.22–1.79 (4H, m, 2 x CH_2), 1.88–1.97 (1H, m), 2.10 (3H, s), 2.79–2.87 (2H, m), 3.99 (2H, d, $J = 5.1$ Hz), 6.82 (1H, s), 6.99–7.19 (4H, m, 4 x CH); ^{13}C NMR (75 MHz, DMSO-d_6) δ: 15.7, 23.8 (2 x CH_3), 28.1, 29.3, 29.9, 33.5, 57.4, 118.8, 119.5, 124.5, 126.9, 130.2, 148.2, 149.4, 171.4, 171.7, 179.5. Anal. Calcd for $C_{20}H_{25}N_3O_5$: C, 62.00; H, 6.50; N, 10.85; O, 20.65. Found: C, 62.03; H, 6.53; N, 10.83; O, 20.61. MS (ESI, *m*/*z*): 400.21 $[M+Na]^+$.

3.1.25. *(S)-6-Amino-2-(5-(5-isopropyl-2-methylphenoxy)-5-oxopentanamido)hexanoic acid (WSCP16)*

Yield: 53%; $R_f = 0.10$, Cyclohexane/EtOAc (1:1); ^{1}H NMR (300 MHz, CD_3OD) δ: 1.21 (6H, d, $J = 6.6$ Hz), 1.42–1.53 (2H, m), 1.62–1.79 (2H, m), 1.83–1.90 (2H, m), 2.31 (2H, t, $J = 6.6$ Hz), 2.11 (3H, s), 2.40 (2H, t, $J = 6.7$ Hz), 2.66 (2H, t, $J = 6.7$ Hz), 2.81–2.94 (3H, m, CH_2 and CH), 4.36–4.40 (1H, m), 6.85 (1H, s), 7.02 (1H, d, $J = 8.1$ Hz), 7.16 (1H, d, $J = 7.5$ Hz); ^{13}C NMR (75 MHz, CD_3OD) δ: 14.5, 20.7, 22.4, 23.0 (2 x CH_3), 26.6, 31.0, 32.6, 33.4, 34.3, 39.1, 52.6, 119.4, 123.7, 127.1, 130.4, 148.0, 149.3, 171.8, 173.9, 179.9. Anal. Calcd for $C_{21}H_{32}N_2O_5$: C, 64.26; H, 8.22; N, 7.14; O, 20.38. Found: C, 64.28; H, 8.18; N, 7.17; O, 20.38. MS (ESI, *m*/*z*): 393.11 $[M+H]^+$.

3.1.26. *(S)-3-(1H-Imidazol-4-yl)-2-(5-(5-isopropyl-2-methylphenoxy)-5-oxopentanamido)propanoic acid (WSCP17)*

Yield: 42%; $R_f = 0.10$, Cyclohexane/EtOAc (1:1); ^{1}H NMR (300 MHz, CD_3OD) δ: 1.20 (6H, d, $J = 7.2$ Hz), 1.21–1.80 (2H, m), 2.07 (3H, s), 2.33–2.41 (2H, m), 2.62–2.70 (2H, m), 2.81–2.94 (3H, m, CH and CH_2), 4.35–4.41 (1H, m), 6.83 (1H, s), 6.97–7.04 (1H, m), 7.12–7.18 (1H, m); ^{13}C NMR (75 MHz, CD_3OD) δ: 15.6, 20.6, 23.7 (2 x CH_3), 29.7, 30.2, 33.4, 35.8, 57.7, 118.7, 119.6, 124.3, 126.8, 130.1, 136.4, 148.3, 149.5, 171.3, 171.5, 179.4. Anal. Calcd for $C_{21}H_{27}N_3O_5$: C, 62.83; H, 6.78; N, 10.47; O, 19.93. Found: C, 62.79; H, 6.77; N, 10.49; O, 19.94. MS (ESI, *m*/*z*): 402.21 $[M+H]^+$.

3.1.27. *Synthesis of compounds 10–11*

A solution of **WSCP4** or **WSCP8** (1.80 mmol), TEA (0.25 mL, 1.80 mmol), and IBCF (0.23 mL, 1.80 mmol) in dry THF (10 mL) was stirred for 20 min at −15 °C. Afterwards, a solution of N-Boc-ethylenediamine in dry THF (5 mL) was dropped into the reaction mixture and stirred for further 3 h at 0 °C, then 15 h at room temperature, to give derivative **10** or **11**, respectively. After filtration and evaporation of the solvent, the crude residue was purified on silica gel with DCM/EtOAc (8:2) or $CHCl_3$/MeOH (95:5), as eluent systems to provide compounds **10** or **11**, respectively, in good yields.

3.1.28. *5-Isopropyl-2-methylphenyl 4-((2-((tert-butoxycarbonyl)amino)ethyl)amino)-4-oxobutanoate (10)*

Yield: 36%; $R_f = 0.59$, DCM/EtOAc (8:2); ^{1}H NMR (300 MHz, $CDCl_3$) δ: 1.20 (6H, d, $J = 7$ Hz), 1.48 (9H, s), 2.12 (3H, s), 2.64 (2H, t, $J = 6.9$ Hz), 2.87 (2H, t, $J = 7.2$ Hz), 2.96–3.05 (1H, m), 3.22–3.28 (2H, m), 3.47–3.54 (2H, m), 6.85 (1H, s), 7.00 (1H, d, $J = 7.5$ Hz), 7.18 (1H, d, $J = 7.5$ Hz); ^{13}C NMR (75 MHz, $CDCl_3$) δ: 15.2, 23.3 (2 x CH_3), 28.4 (3 x CH_3), 31.2, 32.5, 34.9, 39.4, 40.2, 80.6, 120.7, 123.9, 127.4, 130.0, 148.5, 151.1, 157.8, 171.8, 172.2.

5-Isopropyl-2-methylphenyl 5-((2-((tert-butoxycarbonyl)amino)ethyl)amino)-5-oxopentanoate (11). Yield: 36%; $R_f = 0.59$, DCM/EtOAc (8:2); ^{1}H NMR (300 MHz, $CDCl_3$) δ: 1.20 (6H, d, $J = 6.9$ Hz), 1.40 (9H, s), 2.03–2.11 (5H, m, CH_3 and CH_2), 2.29 (2H, t, $J = 6.9$ Hz), 2.61 (2H, t, $J = 7.2$ Hz), 2.80–2.86 (1H, m), 3.20–3.24 (2H, m), 3.28–3.32 (2H, m), 6.82 (1H, s), 6.99 (1H, d, $J = 7.5$ Hz), 7.11 (1H, d, $J = 7.5$ Hz); ^{13}C NMR (75 MHz, $CDCl_3$) δ: 15.8, 20.8, 23.8 (2 x CH_3), 28.3 (3 x CH_3), 33.2, 33.5, 35.2, 40.2, 40.5, 78.6, 119.7, 124.0, 127.0, 130.8, 148.0, 149.1, 167.8, 171.5, 172.8.

3.1.29. *Synthesis of WSCP6 and WSCP10*

A suitable *tert*-butyl ester (**10** or **11**) (0.96 mmol) was dissolved in dry EtOAc (5 mL) and stirred for 1 h at 0 °C under HCl gas. The solvent was then removed under vacuum to quantitatively give the respectively final pure compounds as oils.

3.1.30. *5-Isopropyl-2-methylphenyl 4-((2-aminoethyl)amino)-4-oxobutanoate hydrochloride (WSCP6)*

Yield: 36%; $R_f = 0.59$, DCM/EtOAc (8:2); ^{1}H NMR (300 MHz, $CDCl_3$) δ: 1.21 (6H, d, $J = 7.2$ Hz), 2.10 (3H, s), 2.66 (2H, t, $J = 6.3$ Hz), 2.82–2.87 (1H, m), 2.92 (2H, t, $J = 6.9$ Hz), 3.05 (2H, t, $J = 6$ Hz), 3.46 (2H, t, $J = 5.4$ Hz), 6.86 (1H, s), 7.01 (1H, d, $J = 7.5$ Hz), 7.13 (1H, d, $J = 7.5$ Hz); ^{13}C NMR (75 MHz, $CDCl_3$) δ: 14.5, 22.9 (2 x CH_3), 28.6, 29.7, 33.4, 36.7, 39.4, 119.3, 123.7, 127.1, 130.4, 147.9, 149.2, 171.8, 174.0. Anal. Calcd for $C_{16}H_{25}ClN_2O_3$: C, 58.44; H, 7.66; Cl, 10.78; N, 8.52; O, 14.60. Found: C, 58.49; H, 7.60; Cl, 10.71; N, 8.50; O, 14.69. MS (ESI, *m*/*z*): 329.90 $[M+H]^+$.

3.1.31. *5-Isopropyl-2-methylphenyl 5-((2-aminoethyl)amino)-5-oxopentanoate hydrochloride (WSCP10)*

Yield: 36%; $R_f = 0.59$, DCM/EtOAc (8:2); ^{1}H NMR (300 MHz, $CDCl_3$) δ: 1.13 (6H, d, $J = 7.2$ Hz), 1.82–187 (2H, m), 2.01 (3H, s), 2.21 (2H, t, $J = 6.9$ Hz), 2.58 (2H, t, $J = 7.5$ Hz), 2.79–2.83 (3H, m, CH and CH_2), 3.28 (2H, q, $J = 6$ Hz), 6.88 (1H, s), 7.00 (1H, d, $J = 7.8$ Hz), 7.14 (1H, d, $J = 7.5$ Hz); ^{13}C NMR (75 MHz, $CDCl_3$) δ: 15.8, 20.8, 24.2 (2 x CH_3), 33.1, 33.2, 34.6, 36.9, 39.0, 120.2, 124.2, 127.3, 131.1, 148.0, 149.4, 171.6, 172.5. Anal. Calcd for $C_{17}H_{26}N_2O_3$: C, 66.64; H, 8.55; N, 9.14; O, 15.67. Found: C, 66.59; H, 8.50; N, 9.18; O, 15.73. MS (ESI, *m*/*z*): 344.4 $[M+H]^+$.

3.1.32. *Synthesis of WSCP7 and WSCP11*

A solution of **WSCP4** or **WSCP8** (1.80 mmol), TEA (0.25 mL, 1.80 mmol), and IBCF (0.23 mL, 1.80 mmol) in dry THF (10 mL) was stirred for 20 min at −15 °C. Afterwards, a solution of N,N-dimethylethylenediamine (1.73 mmol) in dry THF (5 mL) was added dropwise into the reaction mixture and stirred for 3 h at 0 °C, and then 15 h at room temperature. After filtration and evaporation of the solvent, the crude product was purified on silica gel with

EtOAc/MeOH (6:4) (**WSCP7**), and DCM/MeOH (95:5) (**WSCP11**) as eluent systems to provide the compounds **WSCP7** and **WSCP11**, respectively, in good yields as oils.

3.1.33. 5-Isopropyl-2-methylphenyl 4-((2-(dimethylamino)ethyl) amino)-4-oxobutanoate hydrochloride (WSCP7)

Yield: 65%; $R_f = 0.74$, $CHCl_3$/MeOH (95:5); ^{1}H NMR (300 MHz, $CDCl_3$) δ: 1.18 (6H, d, $J = 7.2$ Hz), 2.17 (3H, s), 2.31 (6H, s), 2.58–2.63 (6H, m, 3 x CH_2), 2.73–2.85 (1H, m), 3.62 (2H, t, $J = 6.9$ Hz), 6.93 (1H, s), 7.11 (1H, d, $J = 7.5$ Hz), 7.19 (1H, d, $J = 7.5$ Hz); ^{13}C NMR (75 MHz, $CDCl_3$) δ: 15.7, 24.0 (2 x CH_3), 28.1 (2 x CH_2), 33.5, 35.9, 44.8 (2 x CH_3), 55.7, 112.8, 117.5, 121.6, 130.6, 147.9, 154.8, 174.4, 177.7. Anal. Calcd for $C_{18}H_{28}N_2O_3$: C, 67.47; H, 8.81; N, 8.74; O, 14.98. Found: C, 67.51; H, 8.79; N, 8.70; O, 14.99. MS (ESI, *m*/*z*): 321.95 $[M+H]^+$.

3.1.34. 5-Isopropyl-2-methylphenyl 5-((2-(dimethylamino)ethyl) amino)-5-oxopentanoate hydrochloride (WSCP11)

Yield: 65%; $R_f = 0.74$, $CHCl_3$/MeOH (95:5); ^{1}H NMR (300 MHz, $CDCl_3$) δ: 1.14 (6H, d, $J = 6.9$ Hz), 1.80–1.87 (2H, m), 2.02 (3H, s), 2.18–2.28 (2H, m), 2.4 (6H, s), 2.56–2.66 (4H, m, 2 x CH_2), 2.80–2.85 (1H, m), 3.12–3.28 (2H, dq), 6.88 (1H, s), 7.01 (1H, d, $J = 7.5$ Hz), 7.15 (1H, d, $J = 7.5$ Hz);^{13}C NMR (75 MHz, $CDCl_3$) δ: 15.8, 19.3, 24.2 (2 x CH_3), 33.2, 34.6, 35.8, 37.6, 44.4 (2 x CH_3), 57.5, 120.2, 124.2, 127.3, 131.0, 148.0, 149.4, 171.6, 172.1. Anal. Calcd for $C_{19}H_{30}N_2O_3$: C, 68.23; H, 9.04; N, 8.38; O, 14.35. Found: C, 68.13; H, 9.09; N, 8.40; O, 14.37. MS (ESI, *m*/*z*): 335.31 $[M+H]^+$.

3.1.35. Synthesis of WSCP18-20

A solution of CAR (100 mg, 0.67 mmol) in dry acetone (4 mL) was added with K_2CO_3 (1.1 eq.), and the mixture was stirred for 10 min at room temperature. The suitable alkylating agent (3,3-dimethylallyl chloride, geranyl chloride, or *trans*-farnesyl chloride (1.1 eq) was added to the mixture, which was stirred for 4 h at 80 °C. After cooling, the required products were purified by chromatography using CH_2Cl_2/MeOH (95:5) as eluent. **WSCP18**–**20** were obtained as oils in 83–95% yields.

3.1.36. 4-Isopropyl-1-methyl-2-((3-methylbut-2-en-1-yl)oxy) benzene (WSCP18)

Yield: 95%; R*f* = 0.72; ^{1}H NMR (300 MHz, $CDCl_3$) δ: 1.27–1.31 (2 x s, 6H), 1.79–1.84 (m, 6H, $J = 7$ Hz), 2.24 (s, 3H), 2.85–2.95 (sep., 1H, $J = 7$ Hz), 4.57–4.59 (m, 2H), 5.54–5.56 (m, 1H), 6.76–6.79 (m, 2H), 7.08–7.11 (m, 1H); ^{13}C NMR (300 MHz, $CDCl_3$) δ: 15.96, 18.20, 24.18, 25.83, 34.17, 65.02, 110.0, 118.01, 120.54, 124.37, 130.42, 136.99, 147.74, 156.99. Anal. Calcd for $C_{15}H_{22}O$: C, 82.52; H, 10.16; O, 7.33. Found: C, 82.58; H, 10.19; O, 7.23. MS (ESI, *m*/*z*): 218.99 $[M+H]^+$.

3.1.37. (E)-2-((3,7-Dimethylocta-2,6-dien-1-yl)oxy)-4-isopropyl-1-methylbenzene (WSCP19)

Yield: 91%; R*f* = 0.77; ^{1}H NMR (300 MHz, $CDCl_3$) δ: 1.36–1.79 (m, 6H), 1.86–1.90 (m, 3H), 1.91–2.01 (m, 6H), 2.17–2.39 (m, 4H), 2.99–3.06 (sep., 1H, $J = 7.0$ Hz), 4.73–4.75 (m, 2H), 5.27–5.31 (m, 1H), 5.67–5.71 (m, 1H), 6.89–6.90 (m, 2H), 7.20–7.23 (m, 1H); ^{13}C NMR (300 MHz, $CDCl_3$) δ: 16.09, 16.28, 16.77, 17.81, 24.03, 24.11, 24.18, 24.32, 25.82, 26.58, 34.32, 39.73, 65.13, 110.05, 118.12, 120.68, 124.09, 130.56, 131.68, 140.04, 147.74, 157.14. Anal. Calcd for $C_{20}H_{30}O$: C, 83.86; H, 10.56; O, 5.59. Found: C, 83.91; H, 10.51; O, 5.58. MS (ESI, *m*/*z*): 308.96 $[M+Na]^+$.

3.1.38. 4-Isopropyl-1-methyl-2-(((2E,6E)-3,7,11-trimethyldodeca-2,6,10-trien-1-yl)oxy)benzene (WSCP20)

Yield: 83%; R*f* = 0.83; ^{1}H NMR (300 MHz, $CDCl_3$) δ: 1.58 (s, 3H), 1.59 (s, 3H), 1.66 (s, 3H), 1.69–1.72 (m, 6H, $J = 7$ Hz), 1.98–2.02 (m, 4H), 2.12–2.15 (m, 4H), 2.21 (s, 3H), 2.79–2.91 (sep., 1H, $J = 7.0$ Hz), 4.56–4.58 (m, 2H), 5.06–5.12 (m, 2H), 5.49–5.53 (m, 1H), 6.65 (s, 1H), 6.74–6.76 (m, 1H), 7.05–7.07 (m, 1H). ^{13}C NMR (300 MHz, $CDCl_3$) δ: 13.7, 16.16, 16.27, 17.67, 23.88, 25.67, 25.90, 26.72, 33.82, 33.82, 39.64, 65.93, 112.78, 119.78, 123.82, 124.33, 125.30, 130.64, 131.28, 135.33, 141.60, 149.58, 157.44. Anal. Calcd for $C_{25}H_{38}O$: C, 84.69; H, 10.80; O, 4.51. Found: C, 84.63; H, 10.83; O, 4.53. MS (ESI, *m*/*z*): 709.93 $[2M + H]^+$.

3.1.39. Synthesis of WSCP21-23

A solution of CAR (136.5 mg, 0.9 mmol) in DCM (5 mL) was added dropwise to the suitable acid chlorides (3,3-dimethylacryloyl chloride, (2E)-3,7-dimethyl-2,6-octadienoyl chloride, or (R)-citronelloyl chloride (1.17 mmol)), in the presence of Et_3N (118.4 mg, 1.17 mmol). The resulting mixtures were stirred at room temperature for 4–5 h. At the end of the reaction, the corresponding products were extracted with DCM (3 × 10 mL) and the organic fractions were dried and concentrated under reduced pressure, affording the crude products. After silica gel column chromatography was performed with CH_2Cl_2/MeOH (95:5) as eluent, **WSCP21**–**23** were obtained as oils in good yield.

3.1.40. 5-Isopropyl-2-methylphenyl 3-methylbut-2-enoate (WSCP21)

Yield: 90%; R*f* = 0.64; ^{1}H NMR (300 MHz, $CDCl_3$) δ: 1.21–1.30 (m, 6H), 1.95–1.99 (m, 6H, $J = 7$ Hz), 2.21 (s, 3H), 2.8–3.07 (sep., 1H, $J = 7.0$ Hz), 5.11–5.12 (m, 1H), 6.89–6.91 (m, 1H), 7.13–7.15 (m, 1H), 7.16–7.18 (m, 1H). ^{13}C NMR (300 MHz, $CDCl_3$) δ: 16.24, 20.22, 23.88, 27.2, 33.82, 114.64, 121.75, 123.83, 125.38, 134.33, 150.13, 152.61, 157.66, 165.70. Anal. Calcd for $C_{15}H_{20}O_2$: C, 77.55; H, 8.68; O, 13.77. Found: C, 77.59; H, 8.63; O, 13.79. MS (ESI, *m*/*z*): 255.41 $[M+Na]^+$.

3.1.41. (E)-5-Isopropyl-2-methylphenyl 3,7-dimethylocta-2,6-dienoate (WSCP22)

Yield: 82%; R*f* = 0.70; ^{1}H NMR (300 MHz, $CDCl_3$) δ: 1.22–1.24 (m, 3H), 1.26–1.27 (m, 3H), 1.60 (s, 3H), 1.72–1.76 (m, 6H, $J = 7$ Hz), 2.12–2.16 (m, 4H), 2.18 (s, 3H), 2.88–2.94 (sep., 1H, $J = 7.0$ Hz), 5.13–5.15 (m, 1H), 5.16–5.18 (m, 1H), 6.89–6.88 (m, 1H), 7.02–7.04 (m, 1H), 7.17–7.19 (m, 1H). ^{13}C NMR (300 MHz, $CDCl_3$) δ: 16.24, 17.60, 18.53, 23.88, 26.65, 33.82, 41.10, 114.09, 121.75, 123.70, 123.83, 125.38, 132.30, 134.33, 150.13, 152.61, 158.67, 165.54. Anal. Calcd for $C_{20}H_{28}O_2$: C, 79.96; H, 9.39; O, 10.65. Found: C, 79.90; H, 9.41; O, 10.70. MS (ESI, *m*/*z*): 301.81 $[M+H]^+$.

3.1.42. (R)-5-Isopropyl-2-methylphenyl 3,7-dimethyloct-6-enoate (WSCP23)

Yield: 75%; R*f* = 0.75; ^{1}H NMR (300 MHz, $CDCl_3$) δ: 1.225–1.24 (m, 3H), 1.26–1.275 (m, 3H), 1.60 (s, 3H), 1.72–1.76 (m, 6H, $J = 7$ Hz), 2.15–2.17 (m, 4H), 2.23 (s, 3H), 2.85–2.87 (m, 1H), 2.88–2.94 (sep., 1H, $J = 7.0$ Hz), 5.14–5.17 (m, 1H), 5.87–5.89 (m, 2H), 6.90–6.92 (m, 1H), 7.02–7.04 (m, 1H), 7.15–7.17 (m, 1H). ^{13}C NMR (300 MHz, $CDCl_3$) δ: 16.24, 17.77, 19.49, 23.88, 25.46, 26.0, 29.96, 33.82, 37.21, 42.0, 121.24, 123.83, 124.80, 124.87, 131.14, 132.02, 147.83, 149.94, 172.81. Anal. Calcd for $C_{20}H_{30}O_2$: C, 79.42; H, 10.00; O, 10.58. Found: 79.39; H, 10.02; O, 10.57. MS (ESI, *m*/*z*): 325.46 $[M+Na]^+$.

3.2. Antibacterial activity evaluation

One hundred clinical isolates (including gram-positive, n = 60, and gram-negative, n = 40), were recently collected from human specimens in laboratories in central Italy and used to evaluate the antimicrobial activity of **WSCP1**–**23**. A total of 14 ATCC and NCTC standard strains were used in this study: *Staphylococcus aureus* ATCC 29213, ATCC 43300 and ATCC 700699 (formerly Mu50); *Staphylococcus epidermidis* ATCC 35984 (formerly RP62A) and

HAM892 (an ATCC 35984-derived acriflavin mutant, biofilm defective); *Enterococcus faecalis* ATCC 29212 and NCTC 12201; *Streptococcus pneumoniae* ATCC 49619; *Streptococcus agalactiae* ATCC BAA-611 (formerly 2603 V/R); *Escherichia coli* ATCC 25922 and ATCC 35218; *Klebsiella pneumoniae* ATCC 700603; *Pseudomonas aeruginosa* ATCC 27853; and *Acinetobacter baumannii* ATCC 19606.

Stock solutions of CAR 1% (v/v, 10 mg/mL) were prepared in absolute EtOH, stored at −20 °C and used following dilution. For the susceptibility assay, **WSCP1-23** were stored in water or EtOH at −20 °C, depending on the different solubility properties. The minimal inhibitory concentration (MIC) values of CAR and **WSCP1-23** were determined in Mueller-Hinton II Broth (MHB) and 3% cation-adjusted MHB (CAMHB) for fastidious bacteria by the broth microdilution method according to the Clinical Laboratory Standard Institute guidelines (CLSI, 2014). All drugs were tested at concentrations ranging from 512 to 8 μg/mL. The microplates were incubated at 37 °C for 18–24 h. All experiments were performed in triplicate.

3.3. Biofilm formation assay and antibiofilm activity

Biofilm formation and quantification were assessed by a static assay in microtiter plates, as previously described, using two well-known biofilm-producing reference strains (*S. aureus* ATCC 43300 and *S. epidermidis* ATCC 35984) [30]. Overnight cultures grown in tryptic soy broth (Oxoid, Basingstoke, UK) supplemented with 1% (v/v) glucose (TSBG) were harvested by centrifugation and adjusted to $OD_{650} = 0.1$ (corresponding to ~ 1.0×108 CFU/mL). Ninety-six-well polystyrene flat-bottom microtiter plates (Falcon, Becton Dickinson Labware) were inoculated with 0.2 mL aliquots of the adjusted bacterial suspension, incubated at 37 °C, washed three times in phosphate-buffered saline (PBS), dried at 60 °C for 1 h, and then stained with 0.2 mL of a Hucker's crystal violet (CV) solution for 10 min. After removing the CV, the wells were washed three times with sterile distilled water, inoculated with 0.1 mL of 95% EtOH and shaken for 10 min. Biofilm formation was quantified by measuring the absorbance at 690 nm with a Multiscan Ascent apparatus (Thermo Scientific, Waltham, MA, USA). The optical density (OD) cut-off (ODc) was defined as three standard deviations above the mean OD of the negative control [31].

Biofilm-forming ability was assessed in the presence of different concentrations of CAR and **WSCP18**–**19** (1/2, ¼, and 1/8 × MIC). Briefly, 0.1 mL aliquots of the adjusted bacterial suspensions ($OD_{650} = 0.1$) were transferred to each well containing 0.1 mL of TSBG with different concentrations of substances and the microplates were incubated at 37 °C for 24 h. After incubation, the biomass was estimated as described above (CV assay). All experiments were performed at least in triplicate. The results are shown as the mean ± standard deviations (SD) of two independent experiments.

3.4. Scanning electron microscopy

For morphological studies, the biofilm of ATCC 43300 was directly produced in 4-well Lab-Teck chambers slide (Thermo Scientific) for 24 h. Treated cells were grown in the presence of sub-inhibitory concentrations of **WSCP18** as detailed above. The untreated and **WSCP18**-treated cells were pre-fixed with 2.5% glutaraldehyde in 0.1 M cacodylate buffer (pH 7.3) and post-fixed for 2 h in 1% osmium tetroxide in the same buffer. After washing with PBS, the samples were dehydrated using increasing ethanol concentrations (20%, 40%, 60%, 80%, 95%, and 100%), subjected to a critical point dryer, mounted on SEM stubs and gold-sputtered. SEM observations were performed with a Zeiss Supra 40 scanning electron microscope.

3.5. Antifungal activity determination

Due to the clinical importance of *C. albicans,* minimum fungicidal concentration (MFC) determination was done for **WSCP1-23** (Table 1) according to EUCAST protocols. Briefly, 100 μL *C. albicans* was seeded in a 96-well plate with 0.5 McFarland. One hundred microlitres RPMI 1640 medium supplemented with 2% D-glucose was added to each well, and 100 μL of a diluted antifungal solvent was added with different concentration. The plates were incubated at 37 °C ± 1 without shaking. After incubation for 24 h, the absorbance was measured at 530 nm.

3.6. Disc diffusion assay results

A disc diffusion assay was performed for **WSCP1-23** with *Candida albicans* (ATCC10231), *Candida parapsilosis* (ATCC22019), *Candida glabrata* (ATCC 2001), *Candida tropicalis* (KUEN 1025) and *Candida dubliniensis* (CBS7987). Fluconazole and amphotericin B were used as a positive control. All prodrugs were tested in potato dextrose broth medium with 0.8% agar.

3.7. HPLC-UV assays

The analytical HPLC apparatus consisted of a Waters 600 HPLC pump (Waters Corporation, Milford, MA, USA), equipped with a Waters 2996 photodiode array detector set at a length of 274 nm. The mobile phase was a mixture of H_2O and ACN +0.1% TFA flushing under isocratic conditions with a flow of 1 mL/min, and a Hypersil GOLD C18 column (250 × 4.6 mm) was employed.

3.8. In vitro haemolysis assay

Whole heparinized human blood was freshly collected from a healthy, non-smoking donor and used in the experiments within 3 h of being drawn. The haemolysis assay was carried out following the described protocol [32]. Briefly, the blood sample was mixed with Dulbecco's phosphate-buffered saline (D-PBS), and the erythrocytes were collected via centrifugation at 10016*g* for 5 min and then washed four times with sterile D-PBS solution. For preparation of the stock solution, the isolated erythrocytes were diluted with sterile D-PBS. The compound solutions were prepared in PBS at a concentration of 0.1, 1, 10, 50, 100, 250, or 500 μM, mixed with the diluted erythrocyte suspension and incubated at 37 °C for 4 h. After the incubation period, the mixture was centrifuged at 10016 g for 3 min. The absorbance of the samples was measured by a spectrophotometer at 577 nm with a reference wavelength of 655 nm, and the percentage of haemolysis was calculated. DD H_2O and PBS were used as positive and negative control, respectively.

3.9. Cytotoxicity assessment

Cytotoxicity was determined using the MTT assay. This assay was performed in 48-well plates using human keratinocyte HaCaT cells. The HaCaT cells (10^5 cells/well) were maintained (at 37 °C and with 5% CO_2) in Dulbecco's modified Eagle's medium (DMEM) containing 15% foetal bovine serum, 4 mM L-glutamine, penicillin and streptomycin (at a final concentration of 0.1 mg/mL). After 24 h of culture initiation, the cell cultures were exposed to the WSCP derivatives at 0.1, 1, 10, 25, 50 and 100 μM for an additional 48 h. Cell viability was spectrophotometrically evaluated via monitoring the formation of formazan crystals using commercially available kits (Cayman Chemical®, MI, USA). After 72 h, keratinocyte cells were treated with 0.5 mg/mL MTT for 30 min at 37 °C. After washing, the blue formazan was obtained from the cells with an isopropanol/formic acid (95:5) mixture and then spectrophotometrically

detected at 560 nm. In this cytotoxicity testing, Triton-X-100 (1%) was used as positive control (control^{+}), while the untreated cells were designed as negative control (control^{-}). The density of the formed formazan was evaluated in the control^{-} cells as 100% viability [33,34].

3.10. Solubility and lipophilicity

Solubility was determined as previously reported [35]. The cLogP values calculated using the ACD LogP software package, version 4.55 (Advanced Chemistry Development Inc., Toronto, Canada).

3.11. Stability in gastrointestinal fluids

The simulated gastric and intestinal fluids (SGF and SIF respectively) were prepared according to USP specifications. The drug stock solutions were added to preheated SGF and SIF and placed in a 37 °C shaking water bath. At predetermined time points – (0, 15, 30, and 60 min for SGF and 0, 60, 120, and 180 min for SIF), – 100 μL was deproteinised with 100 μL of ice-cold acetonitrile containing 0.5% v/v of formic acid and placed into micro-centrifuge tubes. The samples were centrifuged at 4 °C and 12000 rpm for 10 min. The supernatant was filtered and analysed by HPLC. The relative difference (RD%) was used to predict the amount of degraded compound in the presence of SGF and SIF during the analysis and was calculated with the following equation:

$$RD = \frac{C_i - C_f}{C_i} \times 100\%$$

where C_i is the amount of drug found at the zero time point and C_f is the amount found at the end of incubation [28].

3.12. Human plasma stability

Human plasma was purchased from 3H Biomedical (Uppsala, Sweden, Europe). Enzymatic hydrolysis, was evaluated by adding the stock drug solution to a pre-heated (37 °C) plasma fraction, previously diluted with 0.02 M phosphate buffer (pH 7.4) to give a final volume of 1 mL (80% plasma). Samples of 100 μL were taken at various times, and 200 μL of 0.01 M HCl in methanol was used to stop the enzymatic activity. After centrifugation for 5 min at 5000 g, the supernatant was analysed by HPLC [36].

3.13. Statistical analysis

The results of biological analysis are presented as the mean ± standard deviation of three repetitions. After performing one-way ANOVA with Duncan's test, the differences between the means obtained from the treated and untreated cells were considered statistically significant at the level of $p < 0.05$.

Notes

The authors declare no conflicts of interest.

Acknowledgment

This study was supported by The Scientific and Technological Research Council of Turkey (TUBITAK) with the project number 215S758 and Italian Ministry of Education, University and Research (University of Chieti-Pescara) FAR 2018.

Appendix A. Supplementary data

Supplementary data to this article can be found online at https://doi.org/10.1016/j.ejmech.2019.05.093.

References

[1] P.D. Gupta, T.J. Birdi, Development of botanicals to combat antibiotic resistance, J. Ayurveda Integr. Med. 8 (2017) 266–275, https://doi.org/10.1016/j.jaim.2017.05.004.
[2] H. Chang, T. Cohen, Y.H. Grad, W.P. Hanage, T.F. O'Brien, M. Lipsitch, Origin and proliferation of multiple-drug resistance in bacterial pathogens, Microbiol. Mol. Biol. Rev. 79 (2015) 101–116, https://doi.org/10.1128/MMBR.00039-14.
[3] M.R. Parsek, P.K. Singh, Bacterial biofilms: an emerging link to disease pathogenesis, Annu. Rev. Microbiol. 57 (2003) 677–701, https://doi.org/10.1146/annurev.micro.57.030502.090720.
[4] B. Parrino, D. Schillaci, I. Carnevale, E. Giovannetti, P. Diana, G. Cirrincione, S. Cascioferro, Synthetic small molecules as anti-biofilm agents in the struggle against antibiotic resistance, Eur. J. Med. Chem. 161 (2019) 154–178, https://doi.org/10.1016/j.ejmech.2018.10.036.
[5] L. Marinelli, A. Di Stefano, I. Cacciatore, Carvacrol and its derivatives as antibacterial agents, Phytochemistry Rev. 17 (2018) 903–921, https://doi.org/10.1007/s11101-018-9569-x.
[6] L. Hall-Stoodley, J.W. Costerton, P. Stoodley, Bacterial biofilms: from the natural environment to infectious diseases, Nat. Rev. Microbiol. 2 (2004) 95–108.
[7] F. Nazzaro, F. Fratianni, L. De Martino, R. Coppola, V. De Feo, Effect of essential oils on pathogenic bacteria, Pharmaceuticals 6 (2013) 1451–1474, https://doi.org/10.3390/ph6121451.
[8] A. La Storia, D. Ercolini, F. Marinello, R. Di Pasqua, F. Villani, G. Mauriello, Atomic force microscopy analysis shows surface structure changes in carvacrol-treated bacterial cells, Res. Microbiol. 162 (2011) 164–172, https://doi.org/10.1016/j.resmic.2010.11.006.
[9] E.J.A. Veldhuizen, J.L.M. Tjeerdsma-Van Bokhoven, C. Zweijtzer, S.A. Burt, H.P. Haagsman, Structural requirements for the antimicrobial activity of carvacrol, J. Agric. Food Chem. 54 (2006) 1874–1879, https://doi.org/10.1021/jf052564y.
[10] N.Y. Saad, C.D. Muller, A. Lobstein, Major bioactivities and mechanism of action of essential oils and their components, Flavour Fragrance J. 28 (2013) 269–279, https://doi.org/10.1002/ffj.3165.
[11] M. Coimbra, B. Isacchi, L. Van Bloois, J.S. Torano, A. Ket, X. Wu, R.M. Schiffelers, Improving solubility and chemical stability of natural compounds for medicinal use by incorporation into liposomes, Int. J. Pharm. (Amst.) 416 (2011) 433–442, https://doi.org/10.1016/j.ijpharm.2011.01.056.
[12] H. Naghdi Badi, M. Abdollahi, A. Mehrafarin, M. Ghorbanpour, M. Tolyat, A. Qaderi, M. Ghiaci Yekta, An overview on two valuable natural and bioactive compounds, thymol and carvacrol, in medicinal plants, J. Med. Plants 16 (2017) 1–32.
[13] D.H. Jornada, G.F. Dos Santos Fernandes, D.E. Chiba, T.R.F. De Melo, J.L. Dos Santos, M.C. Chung, The prodrug approach: a successful tool for improving drug solubility, Molecules 21 (2015) 42, https://doi.org/10.3390/molecules21010042.
[14] K.M. Huttunen, H. Raunio, J. Rautio, Prodrugs - from serendipity to rational design, Pharmacol. Rev. 63 (2011) 750–771, https://doi.org/10.1124/pr.110.003459.
[15] N. Vale, A. Ferreira, J. Matos, P. Fresco, M.J. Gouveia, Amino acids in the development of prodrugs, Molecules 23 (2018), https://doi.org/10.3390/molecules23092318.
[16] Y. Sohma, Y. Hayashi, T. Ito, H. Matsumoto, T. Kimura, Y. Kiso, Development of water-soluble prodrugs of the HIV-1 protease inhibitor KNI-727: importance of the conversion time for higher gastrointestinal absorption of prodrugs based on spontaneous chemical cleavage, J. Med. Chem. 46 (2003) 4124–4135, https://doi.org/10.1021/jm030009m.
[17] E. Skrivanova, M. Marounek, V. Benda, P. Brezina, Susceptibility of *Escherichia coli, Salmonella sp.* and *Clostridium Perfringens* to organic acids and monolaurin, Vet. Med. 51 (2007) 81–88, https://doi.org/10.17221/5524-VETMED.
[18] S. Bröer, S.J. Fairweather, Amino acid transport across the mammalian intestine, Comp. Physiol. 9 (2018) 343–373, https://doi.org/10.1002/cphy.c170041.
[19] A.M. Alhassan, M.I. Abdullahi, A. Uba, A. Umar, Prenylation of aromatic secondary metabolites: a new frontier for development of novel drugs, Trop. J. Pharmaceut. Res. 13 (2014) 307–314, https://doi.org/10.4314/tjpr.v13i2.22.
[20] M. Bodanszky, J.Z. Kwei, Side reactions in peptide synthesis: VII. sequence dependence in the formation of aminosuccinyl derivatives from β-benzyl-aspartyl peptides, Int. J. Pept. Protein Res. 12 (1978) 69, https://doi.org/10.1111/j.1399-3011.1978.tb02869.x.
[21] H.-. Matsumoto, T. Hamawaki, H. Ota, T. Kimura, T. Goto, K. Sano, Y. Hayashi, H. Kiso, 'Double-drugs'— a new class of prodrug form of an HIV protease inhibitor conjugated with a reverse transcriptase inhibitor by a spontaneously cleavable linker, Bioorg. Med. Chem. Lett 10 (2000) 1227–1231, https://doi.org/10.1016/S0960-894X(00)00202-X.
[22] C. Araya-Cloutier, H.M.W. den Besten, S. Aisyah, H. Gruppen, J. Vincken, The position of prenylation of isoflavonoids and stilbenoids from legumes (Fabaceae) modulates the antimicrobial activity against Gram positive pathogens,

Food Chem. 226 (2017) 193–201, https://doi.org/10.1016/j.foodchem.2017.01.026.
[23] A.T.M. Serajuddin, Salt formation to improve drug solubility, Adv. Drug Deliv. Rev. 59 (2007) 603–616, https://doi.org/10.1016/j.addr.2007.05.010.
[24] H. Nikaido, Prevention of drug access to bacterial targets: permeability barriers and active Eefflux, Science 264 (1994) 382–388, https://doi.org/10.1126/science.8153625.
[25] H. Nikaido, Porins and specific diffusion channels in bacterial outer membranes, J. Biol. Chem. 269 (1994) 3905–3908.
[26] A. Nostro, A. Marino, A.R. Blanco, L. Cellini, M. Di Giulio, F. Pizzimenti, G. Bisignano, In vitro activity of carvacrol against staphylococcal preformed biofilm by liquid and vapour contact, J. Med. Microbiol. 58 (2009) 791–797, https://doi.org/10.1099/jmm.0.009274-0.
[27] A. Ahmad, A. Khan, F. Akhtar, S. Yousuf, I. Xess, L.A. Khan, N. Manzoor, Fungicidal activity of thymol and carvacrol by disrupting ergosterol biosynthesis and membrane integrity against candida, Eur. J. Clin. Microbiol. Infect. Dis. 30 (2011) 41–50, https://doi.org/10.1007/s10096-010-1050-8.
[28] E.B. Asafu-Adjaye, P.J. Faustino, M.A. Tawakkul, L.W. Anderson, L.X. Yu, H. Kwon, D.A. Volpe, Validation and application of a stability-indicating HPLC method for the in vitro determination of gastric and intestinal stability of venlafaxine, J. Pharm. Biomed. Anal. 43 (2007) 1854–1859, https://doi.org/10.1016/j.jpba.2006.12.035.
[29] P.G.M. Jochems, J. Garssen, A.M. Van Keulen, R. Masereeuw, P.V. Jeurink, Evaluating human intestinal cell lines for studying dietary protein absorption, Nutrients 10 (2018) 322, https://doi.org/10.3390/nu10030322.
[30] E. Marini, G. Magi, M. Mingoia, A. Pugnaloni, B. Facinelli, Antimicrobial and anti-virulence activity of capsaicin against erythromycin-resistant, cell-invasive Group A Streptococci, Front. Microbiol. (2015) 1281, https://doi.org/10.3389/fmicb.2015.01281.
[31] S. Stepanovic, D. Vukovic, I. Dakic, B. Savic, M. Svabic-Vlahovic, A modified microtiter-plate test for quantification of staphylococcal biofilm Fformation, J. Microbiol. Methods 40 (2000) 175–179, https://doi.org/10.1016/S0167-7012(00)00122-6.
[32] T. Yu, A. Malugin, H. Ghandehari, Impact of silica nanoparticle design on cellular toxicity and hemolytic activity, ACS Nano 5 (2011) 5717–5728, https://doi.org/10.1021/nn2013904.
[33] A. Bouzabata, O. Bazzali, C. Cabral, M.J. Gonçalves, M.T. Cruz, A. Bighelli, C. Cavaleiro, J. Casanova, L. Salgueiro, F. Tomi, New compounds, chemical composition, antifungal activity and cytotoxicity of the essential oil from myrtus nivellei batt. & trab., an endemic species of central Sahara, J. Ethnopharmacol. 149 (2013) 613–620, https://doi.org/10.1016/j.jep.2013.06.054.
[34] S. Laserra, A. Basit, P. Sozio, L. Marinelli, E. Fornasari, I. Cacciatore, M. Ciulla, H. Türkez, F. Geyikoglu, A. Di Stefano, Solid lipid nanoparticles loaded with lipoyl-memantine codrug: preparation and characterization, Int. J. Pharm. (Amst.) 15 (2015) 183–191, https://doi.org/10.1016/j.ijpharm.2015.03.001.
[35] P. Sozio, L. Marinelli, I. Cacciatore, A. Fontana, H. Türkez, G. Giorgioni, A. Di Stefano, New flurbiprofen derivatives: synthesis, membrane affinity and evaluation of in vitro effect on β-amyloid levels, Molecules 18 (2013) 10747–10767, https://doi.org/10.3390/molecules180910747.
[36] L. Marinelli, E. Fornasari, A. Di Stefano, H. Turkez, S. Genovese, F. Epifano, I. Cacciatore, Synthesis and biological evaluation of novel analogues of Gly-L-pro-L-glu (GPE) as neuroprotective agents, Bioorg. Med. Chem. Lett 29 (2019) 194–198, https://doi.org/10.1016/j.bmcl.2018.11.057.